nature genetics

Article

https://doi.org/10.1038/s41588-024-02065-2

The NAT1–bHLH110–CER1/CER1L module regulates heat stress tolerance in rice

Received: 14 March 2024

Accepted: 17 December 2024

Published online: 14 January 2025

Check for updates

Hai-Ping Lu[1,4], Xue-Huan Liu[1,2,4], Mei-Jing Wang[1], Qiao-Yun Zhu[1], Yu-Shu Lyu[1], Jian-Hang Xu[1] & Jian-Xiang Liu[1,3]

Rice production is facing substantial threats from global warming associated with extreme temperatures. Here we report that modifying a heat stress-induced negative regulator, a negative regulator of thermotolerance 1 (NAT1), increases wax deposition and enhances thermotolerance in rice. We demonstrated that the C2H2 family transcription factor NAT1 directly inhibits *bHLH110* expression, and bHLH110 directly promotes the expression of wax biosynthetic genes *CER1/CER1L* under heat stress conditions. In situ hybridization revealed that both *NAT1* and *bHLH110* are predominantly expressed in epidermal layers. By using gene-editing technology, we successfully mutated *NAT1* to eliminate its inhibitory effects on wax biosynthesis and improved thermotolerance without yield penalty under normal temperature conditions. Field trials further confirmed the potential of *NAT1*-edited rice to increase seed-setting rate and grain yield. Therefore, our findings shed light on the regulatory mechanisms governing wax biosynthesis under heat stress conditions in rice and provide a strategy to enhance heat resilience through the modification of NAT1.

The global population is rapidly increasing, leading to a substantial rise in food demand[1]. However, crop production is frequently hindered by the impacts of global climate change[2]. Mathematical modeling suggests that cereal production could experience a decline of 6–7% in yield for every 1 °C increase in environmental temperature[3]. Rice (*Oryza sativa* L.) serves as a staple food for over half of the world's population, but it is highly susceptible to heat stress during both the seedling and reproductive stages[4]. Therefore, there is an urgent need to enhance rice thermotolerance through modern breeding programs to meet the escalating global food demand.

Heat stress has detrimental effects on plant growth and development. For example, high temperature disrupts protein folding in both the cytosol and endoplasmic reticulum (ER), leading to the accumulation of misfolded proteins, reactive oxygen species (ROS) and disruption of organelle integration in plants[5]. However, as plants are immobile, they have developed various strategies to mitigate the damage caused by heat stress. These strategies include heat sensing and signaling, transcriptional regulation and post-translational regulation[4,6,7]. Thermotolerance 3 (*TT3*), a quantitative trait locus (QTL) in rice, consists of two genes, *TT3.1* and *TT3.2* (ref. 8). The thermosensor TT3.1 is an E3 ligase that relocates from plasma membrane to endosome, ubiquitinating the chloroplast precursor protein TT3.2 to prevent stress-induced damages conferred by TT3.2 under heat stress conditions[8,9]. In contrast, NTL3 encodes a rice membrane-associated transcription factor that relocates from plasma membrane to nucleus to regulate the expression of genes involved in ROS detoxification and ER protein folding under heat stress conditions[9,10]. In a recent study, sensing Ca^{2+} transcription factor 1/sensing Ca^{2+} transcription factor 2 (SCT1/SCT2) decodes calcium signals from upstream regulator thermotolerance 2 (TT2) to negatively regulate thermotolerance in rice at the transcriptional level[11]. *TT1* is also a QTL for thermotolerance, first identified in African rice (*Oryza glaberrima*)[12]. TT1 encodes an α2 subunit of the 26S proteasome that is involved in the degradation of cytotoxic denatured proteins; overexpressing *OgTT1* in cultivated rice substantially enhanced thermotolerance[12]. However, it is important to note that stronger stress tolerance often comes at the cost of reduced

[1]State Key Laboratory of Plant Environmental Resilience, College of Life Sciences, Zhejiang University, Hangzhou, China. [2]School of Life Sciences, Fudan University, Shanghai, China. [3]Yuelushan Laboratory of Hunan Province, Changsha, China. [4]These authors contributed equally: Hai-Ping Lu, Xue-Huan Liu. e-mail: jianxiangliu@zju.edu.cn

https://doi.org/10.1038/s41588-024-02065-2

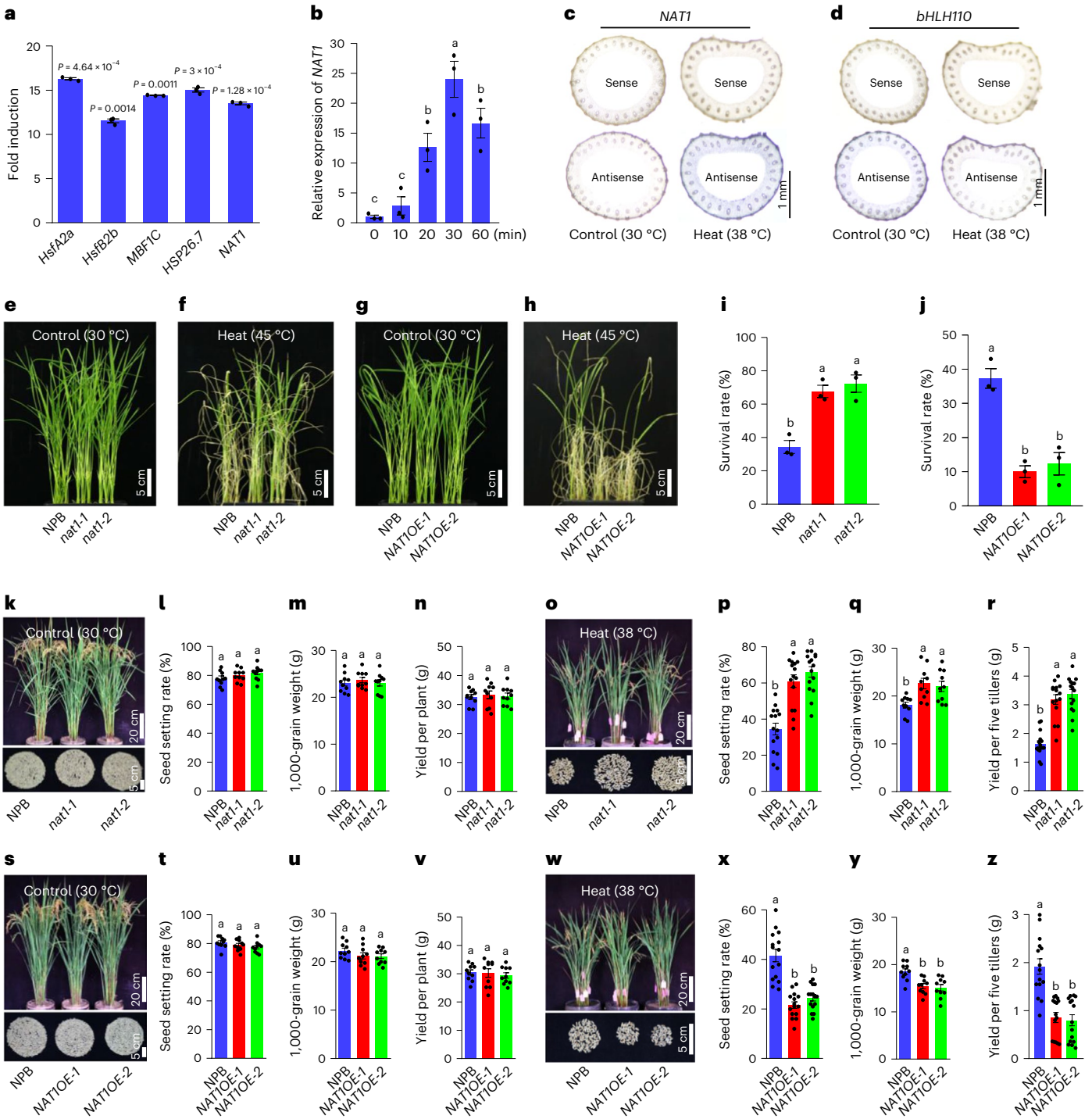

Fig. 1 | NAT1 negatively regulates thermotolerance. a,**b**, Upregulation of *NAT1* expression by AZC and heat stress. Three-day-old NPB plants grown at 30 °C were treated with AZC (5 mM) for 2 h (**a**) or kept either at 30 °C or transferred to 45 °C for the indicated time (**b**), and total seedlings were sampled for RT–qPCR analysis. Fold induction is the $\log_2$ expression value of the AZC-treated sample divided by the nontreated sample, both of which were normalized to that of *Actin*. Relative expression of *NAT1* is the expression level of *NAT1* at 45 °C normalized to that at 30 °C, both of which were normalized to that of *PP2A*. **c**,**d**, Tissue-specific expression of *NAT1* (**c**) and its downstream gene *bHLH110* (**d**). In situ hybridization in the cross-section of NPB stems was performed with antisense and sense probes (control) of *NAT1*/*bHLH110*. **e**–**z**, Phenotypic analysis at seedling stage (**e**–**j**) and reproductive stage (**k**–**z**). In the survival test, NPB, *nat1-1*/*nat1-2* mutants and *NAT1OE-1*/*NAT1OE-2* overexpression plants were grown at 30 °C, subjected to heat stress (45 °C) for 2 days and then recovered at 30 °C for 7 days. The survival rate was calculated. For the thermotolerance test at the reproductive stage, the abovementioned plants were subjected to heat stress at 38 °C for 3 days during flowering and then recovered at 30 °C until maturity. The filled grains per plant (**k**,**s**) or per five panicles (**o**,**w**) were photographed and recorded. Data are presented as mean values ± s.e.m., $n = 3$ in **a**,**b**,**i**,**j**; $n = 10$ in **l**–**n**,**t**–**v**; $n = 15$ in **p**–**r**,**x**–**z**. Two-sided *t*-test was performed (**a**), and the exact *P* values are shown. Different letters indicate significant differences between the two samples, as determined by the Tukey's honestly significant difference (HSD) test ($P < 0.05$) after two-way ANOVA analysis. Scale bars = 1 mm in **c**,**d**; 5 cm in **e**–**h** and **k**,**o**,**s**,**w** for grains; 20 cm in **k**,**o**,**s**,**w** for plant heights.

crop yield[6]. This limitation hinders the widespread use of these tools in molecular breeding. Consequently, additional strategies are needed to improve thermotolerance based on understanding the molecular components of thermotolerance.

In the current study, we have identified an ideal target locus called the negative regulator of thermotolerance 1 (*NAT1*) for enhancing thermotolerance in rice through targeted gene editing. We have discovered that *NAT1* is predominantly expressed in epidermal layers and is highly induced by heat stress. NAT1 has a crucial role in repressing the expression of *bHLH110*, which in turn influences the expression of *ECERIFERUM1* (*CER1*)/CER1-like (*CER1L*), two homologous fatty aldehyde decarbonylase genes responsible for the biosynthesis of wax very-long-chain alkane in rice[13]. By editing the *NAT1* gene in three different variety backgrounds, we have successfully improved thermotolerance. Remarkably, these edited varieties exhibited enhanced tolerance without negative impacts on growth and yield under normal growth conditions. This finding presents a promising alternative approach to ensuring sustainable productivity in the face of global climate change.

Results

NAT1 is a negative regulator of thermotolerance in rice

In our previous microarray experiment, we used the proline analog l-azetidine-2-carboxylic acid (AZC)[14] to induce misfolded proteins in plant cells. We discovered that *NAT1*, along with other well-known heat stress regulators such as *HsfA2a*, *HsfB2b*, *MBF1C* and *HSP26.7* (ref. 15), was substantially upregulated following AZC treatment in wild-type rice Nipponbare (NPB) plants (Fig. 1a). Because heat stress could denature proteins and lead to the accumulation of misfolded proteins[16], we conducted quantitative reverse transcription polymerase chain reaction (RT–qPCR) and revealed that *NAT1* exhibited a strong response to heat stress (Fig. 1b). To examine tissue-specific expression of *NAT1*, we first conducted RT–qPCR with collections of different tissues grown under normal growth temperature (30 °C) and found that *NAT1* was preferentially expressed in roots, stems and developing endosperms (Supplementary Fig. 1a). We then conducted in situ RNA hybridization with stem sections and found that *NAT1* signals were enriched in the epidermal layers and periphery of vascular bundles, which is stronger at 38 °C than that at 30 °C (Fig. 1c). To further investigate its role in heat stress responses, we generated gene-edited *nat1* mutants[17] in the NPB background (Supplementary Fig. 2a). Interestingly, the *nat1-1*/*nat1-2* mutant seedlings exhibited similar growth to NPB plants at 30 °C (Fig. 1e). However, when exposed to 2 days of heat stress (45 °C), the survival rates of *nat1-1*/*nat1-2* mutants were substantially higher compared to NPB plants (Fig. 1f,i). To assess the thermotolerance of *nat1-1*/*nat1-2* mutants at the reproductive stage, we evaluated major agronomic traits such as seed-setting rate, 1,000-grain weight and grain yield. Surprisingly, these mutants showed no significant differences in these traits compared to control plants at 30 °C (Fig. 1k–n). We then subjected both the *nat1-1*/*nat1-2* mutants and NPB plants grown at 30 °C to heat stress (38 °C) starting at flowering for 3 days, followed by a return to 30 °C for recovery. At maturity, we observed that the seed-setting rate, 1,000-grain weight and grain yield of *nat1-1*/*nat1-2* plants were higher than those of NPB plants (Fig. 1o–r).

Additionally, we conducted experiments to overexpress *NAT1* in the NPB background (Supplementary Fig. 2b,c) and examined their heat stress sensitivity. Phenotypic analysis revealed that *NAT1OE-1*/*NAT1OE-2* overexpression plants were more susceptible to heat stress at both the seedling stage (Fig. 1g,h,j) and reproductive stage (Fig. 1s–z) in terms of survival rate, seed-setting rate, 1,000-grain weight and grain yield when compared to the control plants, respectively. Starch accumulation in mature pollen grains is vital for maintaining fertility, especially under heat stress conditions[18]. We stained pollen grain starches with iodine potassium iodide (IKI) and found that the accumulation of starch in pollen grains was higher in *nat1-1* mutant but lower in *NAT1OE-1* plants under heat stress conditions compared to that in NPB; in contrast, the accumulation of starch in pollen grains was similar among these plants under normal conditions (Supplementary Fig. 3a–c). In conclusion, our results demonstrate that NAT1 acts as a negative regulator of thermotolerance in rice. The mutation of *NAT1* confers thermotolerance to rice at both the seedling and reproductive stages.

NAT1 inhibits wax biosynthesis under heat stress conditions

The putative C2H2-type transcription factor encoded by *NAT1* was found exclusively in the nucleus (Fig. 2a). However, NAT1 showed no transcriptional activation activity (Supplementary Fig. 4), so we investigated its potential repression activity. When NAT1 was fused to LexA-DNA-binding domain (LexA-BD), its transcription activation on the LexA operator was reduced (Fig. 2b,c), indicating that NAT1 has transcription repression activity. Furthermore, mutation of the ethylene-responsive element binding factor-associated amphiphilic repression (EAR) domain[19] greatly diminished the repression activity (Fig. 2c).

To understand the role of NAT1 in regulating thermotolerance in rice, we conducted RNA-sequencing (RNA-seq) analysis to compare the transcriptomes of *nat1-1* and NPB seedlings. We identified 497 genes with higher expression and 365 genes with lower expression in *nat1-1* plants than in NPB, specifically at a high temperature (45 °C; Fig. 2d,e and Supplementary Data 1). We considered these 497 genes as *NAT1*-downstream genes because NAT1 is a heat-induced repressor. Kyoto Encyclopedia of Genes and Genomes (KEGG) analysis of these 497 genes revealed enrichment terms of phenylpropanoid biosynthesis, starch and sucrose metabolism, cutin, suberin and wax biosynthesis, fatty acid elongation, etc. (Fig. 2d). We focused on wax biosynthesis in the current study and examined the expression of multiple reported and predicted wax-related genes[11] in our RNA-seq data (Supplementary Data 1) and observed an increased trend in their expression in *nat1-1* mutant compared to NPB under heat stress conditions (Fig. 2f and Supplementary Fig. 5). Among these genes, we focused on two closely related genes (*CER1*/*CER1L*) involved in wax biosynthesis[20,21] and performed quantitative RT–qPCR. The results showed higher expression levels of *CER1*/*CER1L* in *nat1-1*/*nat1-2* plants and lower expression levels in *NAT1OE-1*/*NAT1OE-2* plants compared to NPB under heat stress conditions (Fig. 2g–j), suggesting that NAT1 represses the expression of these wax biosynthetic genes.

Fig. 2 | NAT1 represses downstream genes involved in wax biosynthesis under heat stress conditions. a–c, Subcellular localization and transcription activity assay. The NAT1-green fluorescent protein (NAT1–GFP) fusion protein was transiently co-expressed with the nucleus marker nucleus localized signal-red fluorescent protein (NLS-RFP) in tobacco epidermal leaves and observed under laser microscopy (**a**). For the effector–reporter assay, the native (EAR) or mutated form (ear) of NAT1 was fused to LexA-BD and used as the effector, and the LexA operator lined to the 35S promoter, and the firefly luciferase was used as a reporter (**b** and **c**). **d**,**e**, NAT1-regulated downstream genes (**e**) and their KEGG analysis (**d**). Upregulated genes (FC > 2, $q < 0.05$) in *nat1-1* mutant compared to that in NPB plants were used for drawing the Venn diagram. Circle size represents the number of enriched genes, and the maximum is 15. **f**–**j**, Expression analysis of wax-related genes. NPB, *nat1-1*/*nat1-2* mutants, and *NAT1OE-1*/*NAT1-OE-2* overexpression plants were grown at 30 °C and either kept at 30 °C (control) or transferred to 45 °C for 1 h (HS, heat-stressed; **f**), or for the indicated time period (**g**–**j**). Circles represent genes associated with wax, and the shaded area indicates the 95% confidence interval. In **f**, the red line illustrates the fitted curve based on gene expression patterns and the dashed red line denotes the average value of wax-related genes in NPB plants under heat stress conditions. **k**, Cuticle wax deposition on leaf surfaces. **l**, Wax content in seedlings. Seven-day-old NPB, *nat1-1* mutant and *NAT1OE-1* overexpression plants grown at 30 °C were either kept at 30 °C or transferred to 45 °C for 1 day. Samples were observed under a scanning electron microscope (**k**). Wax content was quantitatively assayed using GC–MS (**l**). C16–C36 represent the number of carbon atoms. Data are presented as mean values ± s.e.m., $n = 3$. Different letters indicate significant differences between the two samples, as determined by the HSD test ($P < 0.05$) after two-way ANOVA analysis. Scale bars = 100 μm (**a**) and 1 μm (**k**).

https://doi.org/10.1038/s41588-024-02065-2

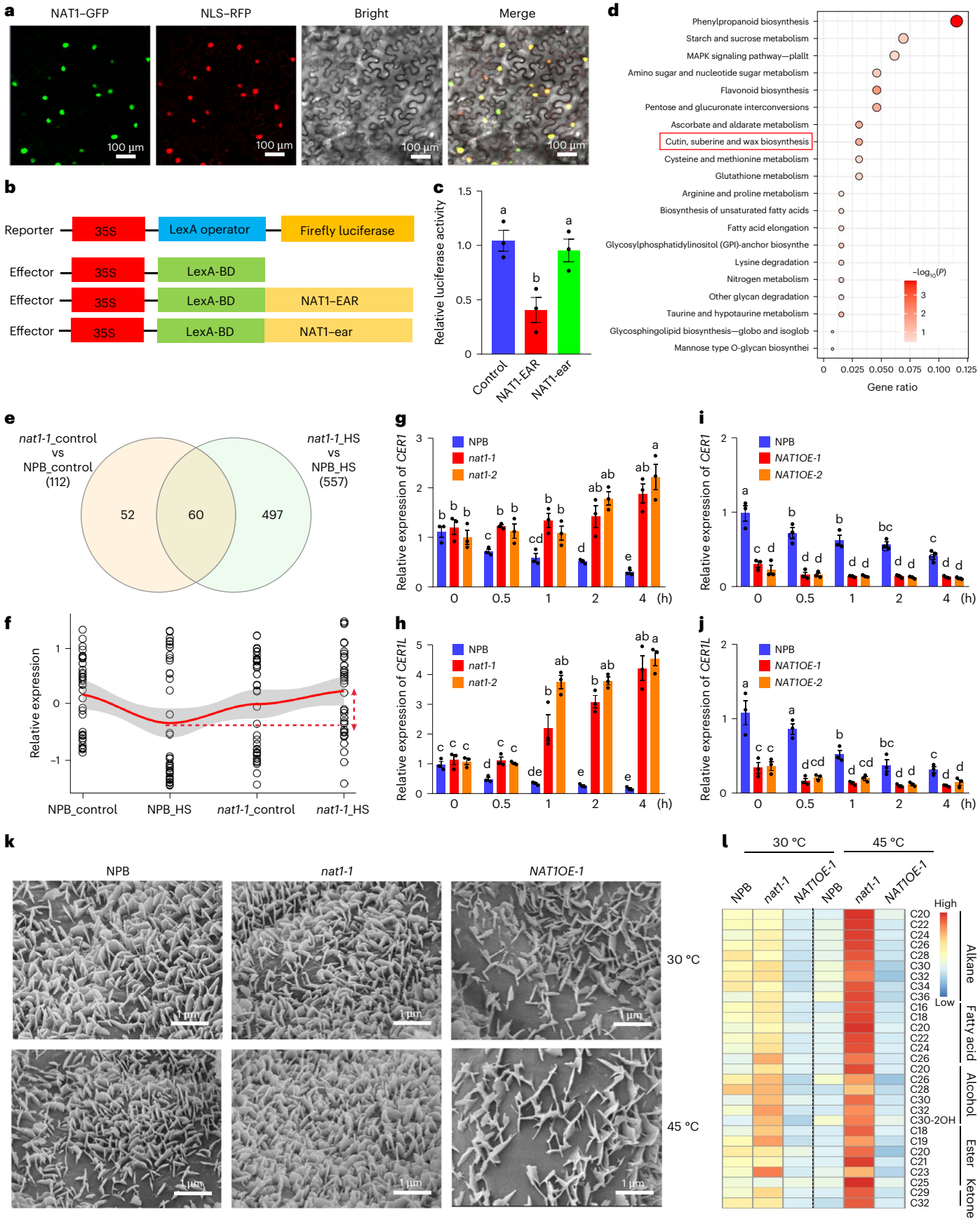

https://doi.org/10.1038/s41588-024-02065-2

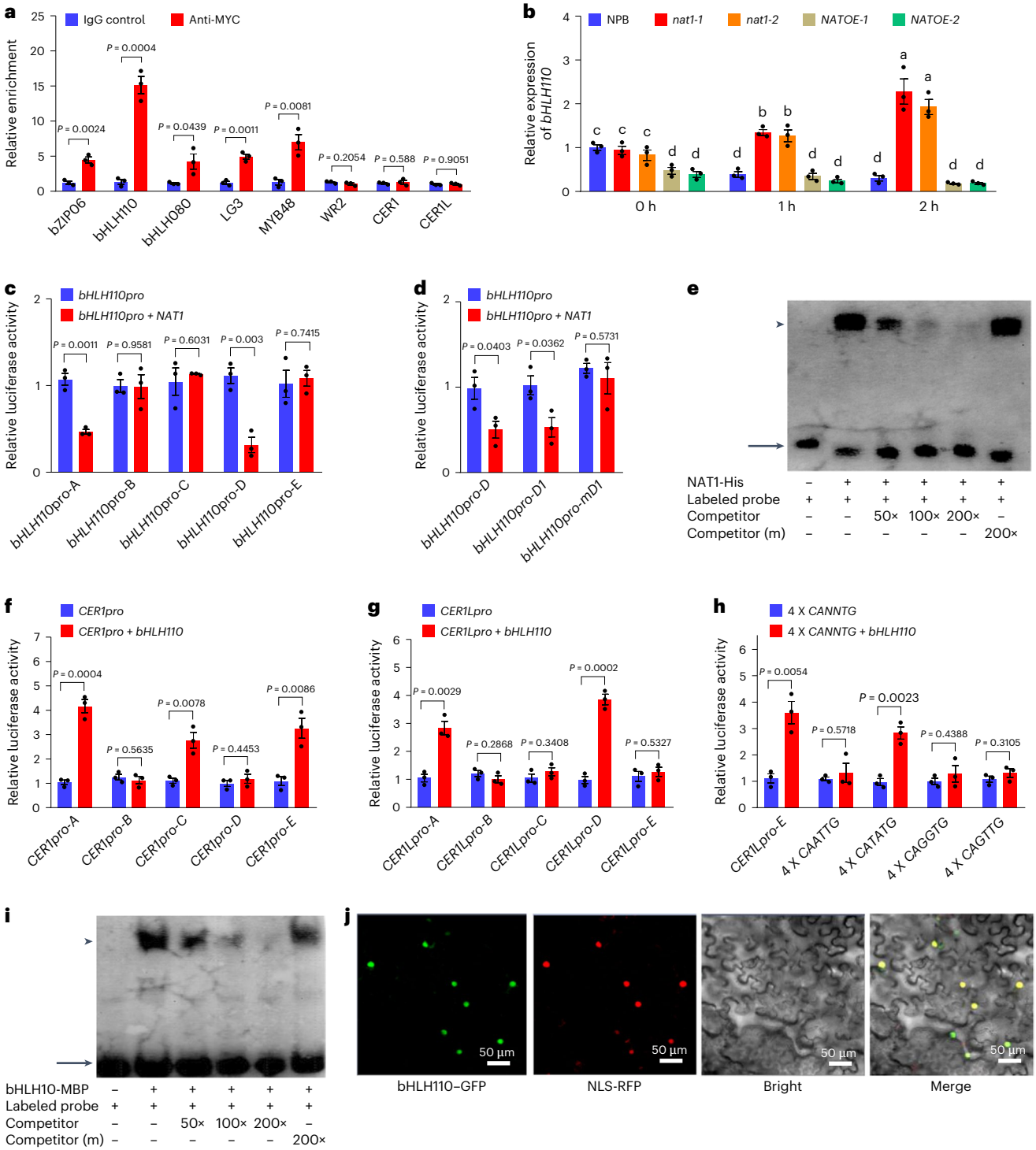

Fig. 3 | NAT1 inhibits the expression of *bHLH110* and bHLH110 promotes the expression of wax biosynthesis genes *CER1*/*CER1L*. **a**–**e**, Inhibition of *bHLH110* expression by NAT1. *NAT1-myc* overexpression plants grown at 30 °C were harvested for ChIP–qPCR (**a**). The expression of *bHLH110* was checked following a period of heat stress treatment (45 °C; **b**). In effector–reporter assays, various segments of *bHLH110* promoter sequences and the 35S promoter were linked to the firefly luciferase and co-expressed with *NAT1* (**c**,**d**). For the EMSA, biotin-labeled A/T-rich probes were incubated with purified NAT1-His protein, while unlabeled native (AGAAAAAG) or mutated (AGGGGGGG) probes were used as competitors (**e**). **f**–**i**, Promotion of *CER1*/*CER1L* expression by *bHLH110*. Different segments of *CER1*/*CER1L* promoter sequences or *cis*-elements were linked to the firefly luciferase and co-expressed with bHLH110 in effector–reporter assays (**f**–**h**). In the EMSA, biotin-labeled E-box (CATATG) probes were incubated with purified bHLH110 protein, and unlabeled native or mutated (CAAAAG) E-box probes were used as competitors (**i**). The relative luciferase activity was determined by normalizing the firefly luciferase activity to the Renilla luciferase activity (internal control), which was then normalized to the vector control. **j**, Subcellular localization. The bHLH110–GFP fusion protein was transiently co-expressed with the nucleus marker NLS-RFP in tobacco epidermal leaves and observed under laser microscopy. Scale bars = 50 μm. **k**,**l**, The expression of *CER1* (**k**) and *CER1L* (**l**) in *bhlh110-1*/*bhlh110-2* mutants and *bHLH110OE-1*/*bHLH110OE-2* overexpression plants subjected to heat stress treatment (45 °C) for the indicated time. Data are presented as mean ± s.e.m., $n = 3$. Two-sided *t*-test was performed (**a**,**c**,**d**,**f**–**h**), and the exact *P* values are shown. Different letters indicate significant differences between the two samples, as determined by the HSD test ($P < 0.05$) after two-way ANOVA analysis. Arrowhead and arrow point to the position of shifted bands and free probes, respectively in **e** and **i**.

To further investigate the role of NAT1 on wax biosynthesis, we examined the surface features of leaves, including cuticle flaky and amorphous wax crystals, using scanning electron microscopy. Under normal temperature conditions (30 °C), the leaf surfaces of NPB and *nat1-1* were densely covered with wax crystals, while the wax density in *NAT1OE-1* plants was lower compared to that in NPB plants (Fig. 2k). In contrast, under high-temperature conditions (45 °C), the wax crystal density of *nat1-1* plants was much higher, while that of *NAT1OE-1* plants was much lower compared to NPB (Fig. 2k). To validate these observations with quantification, we extracted wax compounds from plants and analyzed them using gas chromatography–mass spectrometry (GC–MS). The results showed that the level of known wax-related components (including alkanes, esters, fatty acids and alcohols) was substantially higher in *nat1-1* plants and lower in *NAT1OE-1* plants compared to NPB (Fig. 2l and Supplementary Fig. 6). Together, these findings provide evidence that NAT1 negatively regulates wax biosynthesis under heat stress conditions.

NAT1 directly represses *bHLH110* expression

We investigated whether NAT1 directly represses the expression of *CER1*/*CER1L* by performing chromatin immunoprecipitation–quantitative PCR (ChIP–qPCR). Our results showed that neither the *CER1* promoter nor the *CER1L* promoter was enriched by NAT1 (Fig. 3a). To further explore this, we screened putative transcription factors from the list of differently expressed genes between *nat1-1* and NPB (Supplementary Data 1) and found that the *bHLH110* promoter was highly enriched by NAT1 (Fig. 3a). This finding was consistent with the observation that the expression of *bHLH110* was increased in *nat1-1*/*nat1-2* mutants under heat stress conditions and decreased in *NAT1OE-1*/*NAT1OE-2* overexpression plants compared to NPB (Fig. 3b). Furthermore, the tissue-specific expression pattern of *bHLH110* was correlated to that of *NAT1* (Fig. 1c,d and Supplementary Fig. 1a,b). We also examined the expression of other reported wax-related regulatory genes in rice[11] and found that *TT2*/*SCT1*/*SCT2* expression remained unchanged in *nat1-1*/*nat1-2* mutants and *NAT1OE-1*/*NAT1OE-2* overexpression plants (Supplementary Fig. 7). However, the expression of the wax biosynthesis regulator *Wax synthesis regulatory 2* (*WR2*) downstream of TT2/SCT1/SCT2 was increased in *nat1-1*/*nat1-2* mutants and decreased in *NAT1OE-1*/*NAT1OE-2* overexpression plants (Supplementary Fig. 7). Interestingly, the *WR2* promoter was not enriched by NAT1 (Fig. 3a), suggesting that NAT1 indirectly regulates *WR2* expression. Therefore, we focused on bHLH110 for further study. To investigate the repression of the *bHLH110* promoter by NAT1, we created reporters by linking the *bHLH110* promoter with a constitutive 35 promoter and the firefly luciferase (Supplementary Fig. 8a). Co-expression of these reporters with the effector NAT1 showed strong repression of the *bHLH110* promoter activity, which was dependent on the region from −631 bp to −267 bp (pbHLH110-D; Fig. 3c and Supplementary Fig. 8a). We identified three similar A/T-rich *cis*-elements within this region using an online prediction program[22] (Supplementary Fig. 8b). Effector–reporter assays using the pbHLH110-D1 fragment (containing AGAAAAAG) confirmed that NAT1 repressed the promoter activity, and mutation of the *cis*-elements abolished this inhibition (Fig. 3d). Electrophoretic mobility shift assay (EMSA) further demonstrated that NAT1 specifically binds to the probes containing the A/T-rich *cis*-elements (Fig. 3e). These results indicate that NAT1 directly binds to the *bHLH110* promoter and represses its expression.

bHLH110 is required for thermotolerance

We generated gene-edited mutants and overexpression plants of *bHLH110* (Supplementary Fig. 9a–c), and the phenotypic analysis showed that the mutants (*bhlh110-1*/*bhlh110-2*) and overexpression plants (*bHLH110OE-1*/*bHLH110OE-2*) had similar growth to NPB plants at 30 °C (Fig. 4a,c,g–j,o–r). However, at 45 °C, the *bhlh110* mutants exhibited increased sensitivity to heat stress (Fig. 4b,e,k–n), while the *bHLH110* overexpression plants showed increased tolerance to heat stress (Fig. 4d,f,s–v) at both the seedling and reproductive stages. Additionally, the wax density and composition were reduced in *bhlh110-1* mutant and increased in *bHLH110OE-1* plants compared to NPB, especially under heat stress conditions (Fig. 4w,x and Supplementary Fig. 10). The accumulation of starch in pollen grains was similar between NPB and *bhlh110-1* or between NPB and *bHLH110OE-1* under normal temperature conditions; however, the accumulation of starch in pollen grains was lower in *nat1-1* mutant but higher in *NAT1OE-1* plants under heat stress conditions compared to that in NPB (Supplementary Fig. 3a–c). These findings support the notion that *bHLH110* is a downstream target of NAT1 and positively regulates rice thermotolerance by affecting wax biosynthesis.

bHLH110 directly promotes the expression of *CER1*/*CER1L*

The expression of *CER1*/*CER1L* was altered in *nat1-1*/*nat1-2* and *NAT1OE-1*/*NAT1OE-2* plants, as shown in Fig. 2g–j. These plants exhibited changes in wax deposition (Fig. 2k,l), leading us to investigate

Fig. 4 | bHLH110 positively regulates thermotolerance and cuticle wax content. **a**–**v**, Phenotypic analysis. For the survival test, NPB, *bhlh110-1*/*bhlh110-2* mutants and *bHLH110OE-1*/*bHLH110OE-2* overexpression plants were grown at 30 °C, subjected to heat stress (45 °C) for 2 days and then recovered at 30 °C for 7 days, and the survival rate was calculated (**a**–**f**). For the thermotolerance test at the reproductive stage, the abovementioned plants were subjected to heat stress at 38 °C for 3 days during flowering and then recovered at 30 °C until maturity (**g**–**v**). The filled grains per plant (**g**,**o**) or per five panicles (**k**,**s**) were photographed and recorded. Data are presented as mean ± s.e.m., $n = 3$ in **e**,**f**; $n = 10$ in **h**–**j**,**p**–**r**; $n = 15$ in **l**–**n**,**t**–**v**. Different letters indicate significant differences between the two samples, as determined by the HSD test ($P < 0.05$) after two-way ANOVA analysis. **w**, Cuticle wax deposition on leaf surfaces. **x**, Wax content in seedlings. Seven-day-old NPB, *bhlh110-1* mutant and *bHLH110OE-1* overexpression plants grown at 30 °C were either kept at 30 °C or transferred to 45 °C for 1 day and then sampled for observation under a scanning electron microscope (**w**) or for quantitative assay by GC–MS to determine wax content (**x**). C16–C36 represent the number of carbon atoms. Scale bars = 5 cm in **a**–**d** for plant height and **g**,**k**,**o**,**s** for grains; 20 cm in **g**,**k**,**o**,**s** for plant heights; 1 μm in **w**.

https://doi.org/10.1038/s41588-024-02065-2

whether bHLH110 directly controls the expression of *CER1*/*CER1L*. We first performed effector–reporter assays (Supplementary Fig. 11a) and revealed that bHLH110 enhanced the activity of the *CER1* promoter in two regions, while it increased the activity of the *CER1L* promoter in one region (Fig. 3f,g). To identify potential *cis*-elements, we focused on the E region of the *CER1* promoter and discovered multiple E-boxes (CANNTG). Subsequently, we linked different forms of the E-box to firefly luciferase and conducted effector–reporter assays. Interestingly, bHLH110 substantially promoted the promoter activity of CATATG (Fig. 3h). Notably, the CATATG *cis*-element is widely present in the

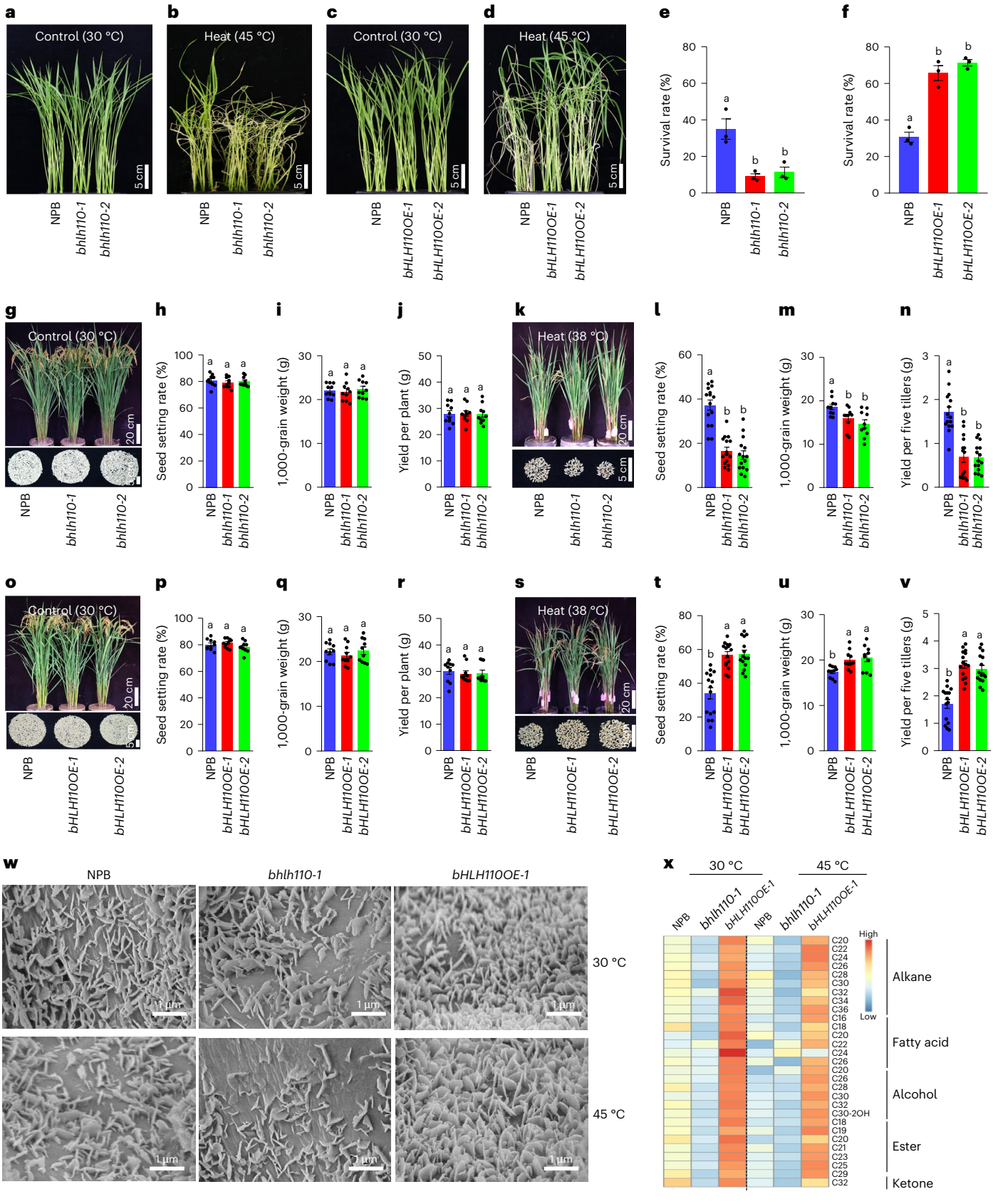

promoters of genes involved in cutin, suberin and wax biosynthesis (Supplementary Fig. 11b). To confirm the direct binding of bHLH110 to the E-box, we performed EMSA experiments and found a direct interaction between bHLH110-MBP and E-box (Fig. 3i). ChIP–qPCR experiment showed that the *CER1/CER1L* promoters were enriched by bHLH110-FLAG (Supplementary Fig. 12). Consistent with its function, bHLH110–GFP was exclusively localized in nucleus (Fig. 3j). Additionally, we examined the expression of *CER1/CER1L* and observed reduced expression in *bhlh110-1/bhlh110-2* mutants, whereas increased expression in *bHLH110OE-1/bHLH110OE-2* overexpression plants compared to NPB plants (Fig. 3k,l). Although the expression of *TT2/SCT1/SCT2* remained largely unchanged, *WR2* expression decreased in *bhlh110-1/bhlh110-2* mutants and increased in *bHLH110OE-1/bHLH110OE-2* overexpression plants (Supplementary Fig. 13). In addition, the *WR2* promoter was enriched by bHLH110 (Supplementary Fig. 12), suggesting that *WR2* is also a direct target of bHLH110. We checked the promoter sequences of *WR2* and found one copy of the E-box. Effector–reporter assays showed that bHLH110 activated the promoter of *WR2* (Supplementary Fig. 14a,b). Interestingly, WR2 activated the promoter of *CER1* but not *CER1L* (Supplementary Fig. 15a,b). Nevertheless, bHLH110 directly binds to the promoter of *CER1/CER1L/WR2* and promotes their expression.

CER1 and CER1L regulate wax deposition and thermotolerance

CER1 was reported to be involved in very-long-chain alkane biosynthesis in rice[21]. To investigate the role of CER1/CER1L in regulating wax biosynthesis and thermotolerance, we created gene-edited mutants of *CER1* and *CER1L* (Supplementary Figs. 16 and 17). Unfortunately, the double mutant (*cer1-1 cer1l-1*) displayed stunted growth and failed to produce any seeds (Supplementary Fig. 18). Consequently, we focused on studying the thermo-sensitivity of the single mutants. The *cer1-1/cer1-2* and *cer1l-1/cer1l-2* mutants exhibited similar growth to NPB plants at 30 °C. However, they showed increased sensitivity to heat stress (45 °C) at the seedling stage, resulting in reduced survival rates (Fig. 5a–f). This sensitivity also extended to the reproductive stage, where the mutants displayed decreased seed-setting rates, 1,000-grain weight and grain yield (Fig. 5k–n,s–v). The accumulation of starch in pollen grains was reduced in *cer1-1/cer1l-1* plants under heat stress conditions compared to that in NPB plants (Supplementary Fig. 3a–c). Notably, the major agronomic traits of *cer1-1/cer1-2* and *cer1l-1/cer1l-2* plants grown at 30 °C were comparable to those of the control plants (Fig. 5g–j,o–r). These findings strongly support the role of CER1 and CER1L as positive regulators of rice thermotolerance. Additionally, we examined the wax deposition and composition of these plants grown at both 30 °C and 45 °C. Consistent with the phenotypic data, the wax density and composition were reduced in *cer1-1/cer1l-1* mutants compared to NPB, particularly under heat stress conditions (Fig. 5w–y and Supplementary Figs. 19 and 20). We also checked the tissue-specific expression of *CER1/CER1L*. They were dominantly expressed in leaves, anthers and endosperms (Supplementary Fig. 1c,d). In situ hybridization studies showed that they are expressed in epidermis and vicinity of vasculature bundles (Supplementary Fig. 1e,f), which agrees with their roles in wax deposition. Thus, CER1 and CER1L are essential for thermotolerance in rice through their regulation of wax biosynthesis.

NAT1-regulated thermotolerance relies on *bHLH110/CER1/CER1L*

To determine if the enhanced thermotolerance in *nat1* mutants relies on bHLH110 or *CER1* or *CER1L*, we created loss-of-function mutants of *bHLH110/CER1/CER1L* in the *nat1-2* background, respectively (Supplementary Figs. 21, 24 and 25). These mutant plants exhibited similar growth to NPB at 30 °C (Fig. 6a–d,i–l,q–t). In contrast to the thermotolerant phenotype of the *nat1-2* mutant, the abovementioned mutants showed heat-sensitive phenotypes (Fig. 6e–h,m–p,u–x). Additionally, mutation of *bHLH110/CER1/CER1L* in the *nat1-2* background also suppressed the enhanced wax accumulation phenotype of the *nat1-2* mutant (Supplementary Figs. 22a,b, 23 and 26). Overall, these genetic analyses support the idea that *nat1*-mediated thermotolerance requires downstream regulators such as bHLH110 and CER1/CER1L involved in wax biosynthesis.

NAT1 has natural variations which diverge between subspecies

To identify natural alleles of *NAT1*, we conducted haplotype analysis on 4,726 rice accessions, including *indica*, *aus*, *japonica* and intermediate varieties. Our analysis revealed only four single-nucleotide polymorphisms (SNPs) in the coding sequence (CDS) region of *NAT1* (Fig. 7a). In contrast, the 2-kb promoter sequence contained 38 SNPs and 19 insertions/deletions (InDels), the 5′ untranslated region (UTR) had 2 SNPs and the 3′ UTR had 7 SNPs and 3 InDels (Fig. 7a and Supplementary Data 2). Excluding synonymous mutations, three major haplotypes (Hap1–Hap3) were classified based on three SNPs in the CDS region. Hap1 and Hap2 accessions accounted for 98.86% of the 4,726 rice accessions analyzed. Furthermore, Hap1 accessions were primarily found in *japonica*/Geng, while Hap2 accessions were predominantly identified in *indica*/Xian (Fig. 7b). Additionally, compared to Hap1 accessions, Hap3 accessions differed only in the amino acid at position 94, which was similar to that in the examined wild rice species except for *Oryza rufipogon* (Fig. 7c).

Japonica and *indica* are two subspecies that are distributed in distinct ecological regions and have contrasting phenotypes with different heat sensitivity[23]. To compare the functional divergence of Hap1 and Hap2, we performed microscale thermophoresis (MST) assays. Compared to the GFP-His control, both $NAT1^{Japonica}$–GFP-His and $NAT1^{Indica}$–GFP-His bind to *bHLH110*-promoter DNA, and the dissociation constant (K_d) was similar (same order of magnitude) between $NAT1^{Japonica}$–GFP-His and $NAT1^{Indica}$–GFP-His (Supplementary Fig. 27a,b). Further effector–reporter assays using different alleles of NAT1 as the effector showed that both $NAT1^{Japonica}$ and $NAT1^{Indica}$ repressed the *bHLH110* promoter activity to a similar extent (Supplementary Fig. 27c). Thus, these results indicate that the functional divergence between Hap1 and Hap2 is very limited. However, the association of other natural variations in *NAT1* with heat stress sensitivity needs to be investigated in the future.

We also found 10 SNPs in the CDS region, 62 SNPs and 20 InDels in the 2-kb promoter sequences, 3 SNPs and 2 InDels in the 5′ UTR and 2 SNPs in the 3′ UTR of *bHLH110* (Fig. 7d and Supplementary Data 2). Excluding synonymous mutations, six major haplotypes (Hap1–Hap6) were classified based on five SNPs in the CDS region (Fig. 7d). Hap1 accessions accounted for 89.55% of the 4,726 rice accessions analyzed. Furthermore, *indica* accounted for the majority of Hap1 accessions at 64.01%, followed by *japonica* at 26.37% (Fig. 7e). Additionally, compared to Hap1 accessions, Hap2 accessions, which have a stop-gained mutation, were predominantly identified in *japonica* (Fig. 7e). For Hap1, there was no difference in the five SNPs in the CDS region between cultivated rice and the examined wild rice species except *Oryza barthii* (Fig. 7f). The Hap2 allele of *bHLH110* is a loss-of-function allele. Whether Hap2 and other natural variations in *bHLH110* are associated with higher heat sensitivity is worth investigating in the future.

To check whether *NAT1* or *bHLH110* has undergone domestication selection, we performed nucleotide diversity (π) analysis of the 2-Mb region spanning the CDS region of *NAT1/bHLH110*. The π values of Geng/*japonica* were slightly lower than those of wild rice, while the π values of Xian/*indica* were similar to those of wild rice for *NAT1*, and the π values for each comparison were similar for *bHLH110* (Supplementary Fig. 28a,c), suggesting that neither *NAT1* nor *bHLH110* has undergone domestication selection, which is agreed with previous reports[24]. Furthermore, we examined *NAT1/bHLH110* evolution by calculating the level of population differentiation index (F_{ST}) in the nearby region of *NAT1/bHLH110* between different species/subspecies. The results showed that F_{ST} level was higher between *japonica* and *indica* than between wild rice and *japonica* or between wild rice and *indica* in the

https://doi.org/10.1038/s41588-024-02065-2

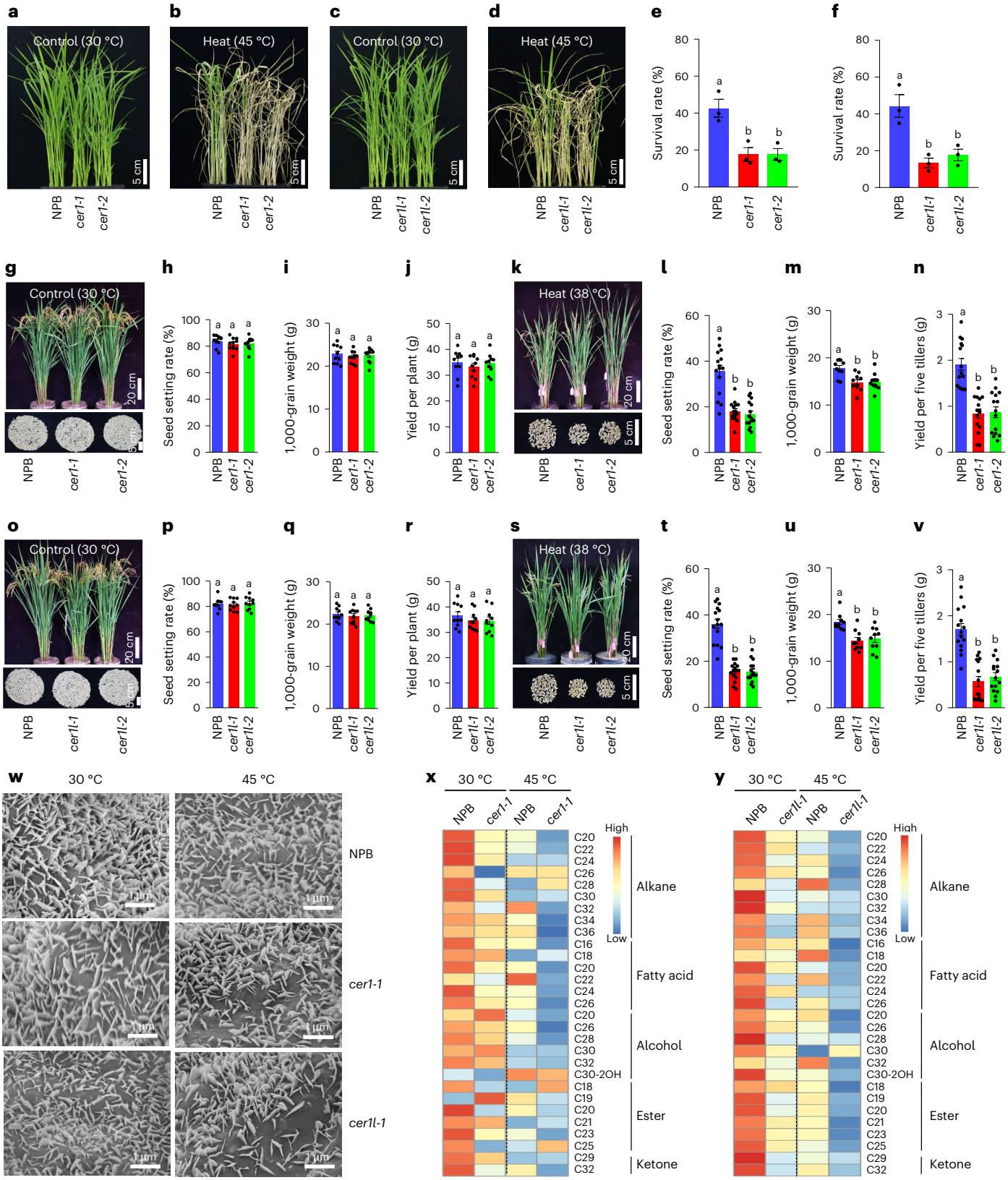

Fig. 5 | CER1-/CER1L-mediated wax deposition is crucial for thermotolerance. **a**–**v**, Phenotypic analysis. In the survival test, NPB, *cer1-1*/*cer1-2* mutants and *cer1l-1*/*cer1l-2* mutants were grown at 30 °C, subjected to heat stress (45 °C) and then recovered at 30 °C for 7 days. The survival rate was calculated based on this test (**a**–**f**). For the thermotolerance test at the reproductive stage, the abovementioned plants were subjected to heat stress at 38 °C during flowering and then recovered at 30 °C until maturity (**g**–**v**). The filled grains per plant (**g**,**o**) or per five panicles (**k**,**s**) were photographed and recorded. Data are presented as mean ± s.e.m., $n = 3$ in **e**,**f**; $n = 10$ in **h**–**j**,**p**–**r**; $n = 15$ in **l**–**n**,**t**–**v**. Different letters indicate significant differences between the two samples, as determined by the HSD test ($P < 0.05$) after two-way ANOVA analysis. **w**, Cuticle wax deposition on leaf surfaces. **x**,**y**, Wax content in seedlings. Seven-day-old NPB, *cer1-1* mutant and *cer1l-1* mutant grown at 30 °C were either kept at 30 °C or transferred to 45 °C for 1 day and sampled for observation under a scanning electron microscope (**w**). Wax content was determined by GC–MS (**x**,**y**). C16–C36 represent the number of carbon atoms. Scale bars = 5 cm in **a**–**d** for plant heights and **g**,**k**,**o**,**s** for grains; 20 cm in **g**,**k**,**o**,**s** for plant heights; 1 μm in **w**.

https://doi.org/10.1038/s41588-024-02065-2

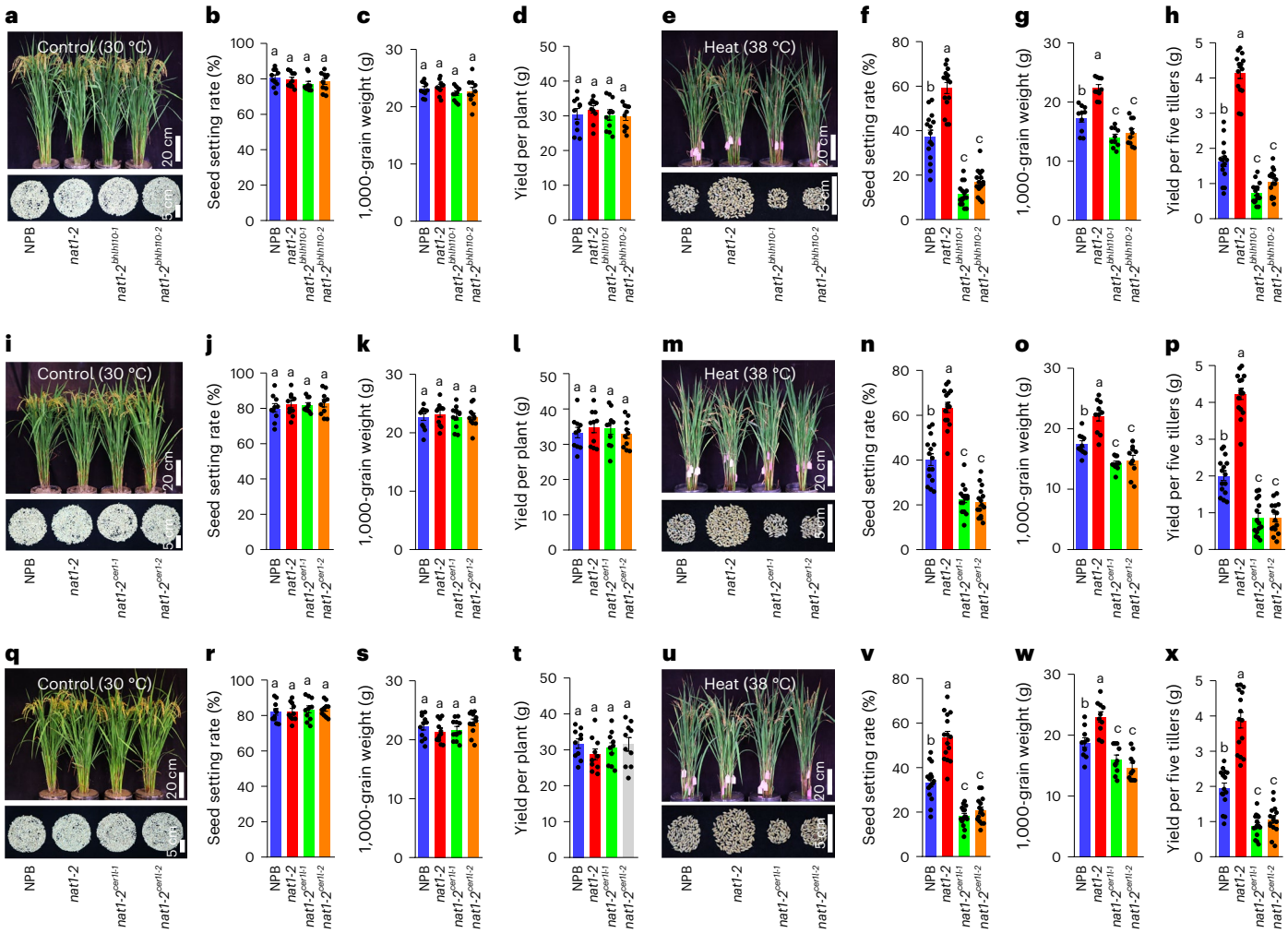

Fig. 6 | *nat1*-conferred thermotolerance requires *bHLH110* and *CER1*/*CER1L*. **a**–**x**, Phenotypic analysis at reproductive stage. NPB, *nat1-2* mutant, *bhlh110* mutants in *nat1-2* background (*nat1-2*$^{bhlh110\text{-}1}$/*nat1-2*$^{bhlh110\text{-}2}$), *cer1* mutants in *nat1-2* background (*nat1-2*$^{cer1\text{-}1}$/*nat1-2*$^{cer1\text{-}2}$) and *cer1l* mutant in *nat1-2* background (*nat1-2*$^{cer1l\text{-}1}$/*nat1-2*$^{cer1l\text{-}2}$) were subjected to heat stress (38 °C) during flowering and then recovered at 30 °C until maturity. The filled grains per plant (**a**,**i**,**q**) or per five panicles (**e**,**m**,**u**) were photographed and recorded. Data are presented as mean ± s.e.m., $n = 10$ in **b**–**d**,**j**–**l**,**r**–**t**; $n = 15$ in **f**–**h**,**n**–**p**,**v**–**x**. Different letters indicate significant differences between the two samples, as determined by the HSD test ($P < 0.05$) after two-way ANOVA analysis. Scale bars = 5 cm in **a**,**e**,**I**,**m**,**q**,**u** for grains; 20 cm in **a**,**e**,**I**,**m**,**q**,**u** for plant heights.

NAT1 gene (Supplementary Fig. 28b), while the F_{ST} values between different species/subspecies were similar and low in the *bHLH110* locus (Supplementary Fig. 27d), indicating that *NAT1* has high sequence divergence between *japonica* and *indica*.

Gene editing of *NAT1* increases thermotolerance in rice

To determine if editing *NAT1* could improve thermotolerance in other rice cultivars, aside from NPB (Fig. 1), we selected Songzaoxiang no. 1 (SZX) and Yuzhenxiang (YZX) as the recipients for transformation. SZX, an early maturing variety, is widely cultivated in the Changjiang Delta region of China as 'Guo-Qing-Dao'. However, its yield is negatively impacted by high temperatures occurring during the flowering and seed-setting stage. Therefore, enhancing thermotolerance in SZX is crucial for early sowing and for maximizing its economic benefits. On the other hand, YZX is a suitable variety for ratoon rice production, where a single sowing yields two harvests, saving labor in southern China. Successful ratoon rice production requires improved thermotolerance during both the reproductive and seedling stages. Through our research, we generated loss-of-function mutants of *NAT1* in both SZX and YZX backgrounds (Supplementary Fig. 29) and found that these *nat1* mutants also exhibited greater tolerance to heat stress at both the seedling (Fig. 8a–f) and reproductive stages (Fig. 8g–v), without significant decrease in yield under normal temperature conditions. In addition, editing *NAT1* does not reduce regeneration capacity, as new shoots are produced in *nat1-5* mutant plants under both normal and high-temperature conditions (Supplementary Fig. 30). To evaluate the potential of *NAT1*-editing for breeding purposes, we conducted preliminary field trials in Huzhou and Quzhou of Zhejiang province, growing SZX and *nat1-3* (SZX background). In Quzhou, the plants were transplanted 16 days earlier than in Huzhou, and the number of high-temperature days (above 34 °C) was larger in Quzhou than in Huzhou during the growth period (Supplementary Fig. 31a,b). Our findings revealed that the *nat1–3* mutant exhibited a higher seed-setting rate, 1,000-grain weight and grain yield per plot compared to the control plants in both geographic locations (Fig. 8w,x), with a greater yield increase observed in Quzhou compared to Huzhou (Fig. 8w,x). Therefore, editing *NAT1* holds substantial potential for breeding environmental-resilient rice cultivars.

Discussion

Understanding the molecular mechanisms underlying thermotolerance in plants is crucial for developing temperature-resilient crops. In this study, we have identified a regulatory module, NAT1–bHLH110–CER1/CER1L, which controls wax biosynthesis and thermotolerance

https://doi.org/10.1038/s41588-024-02065-2

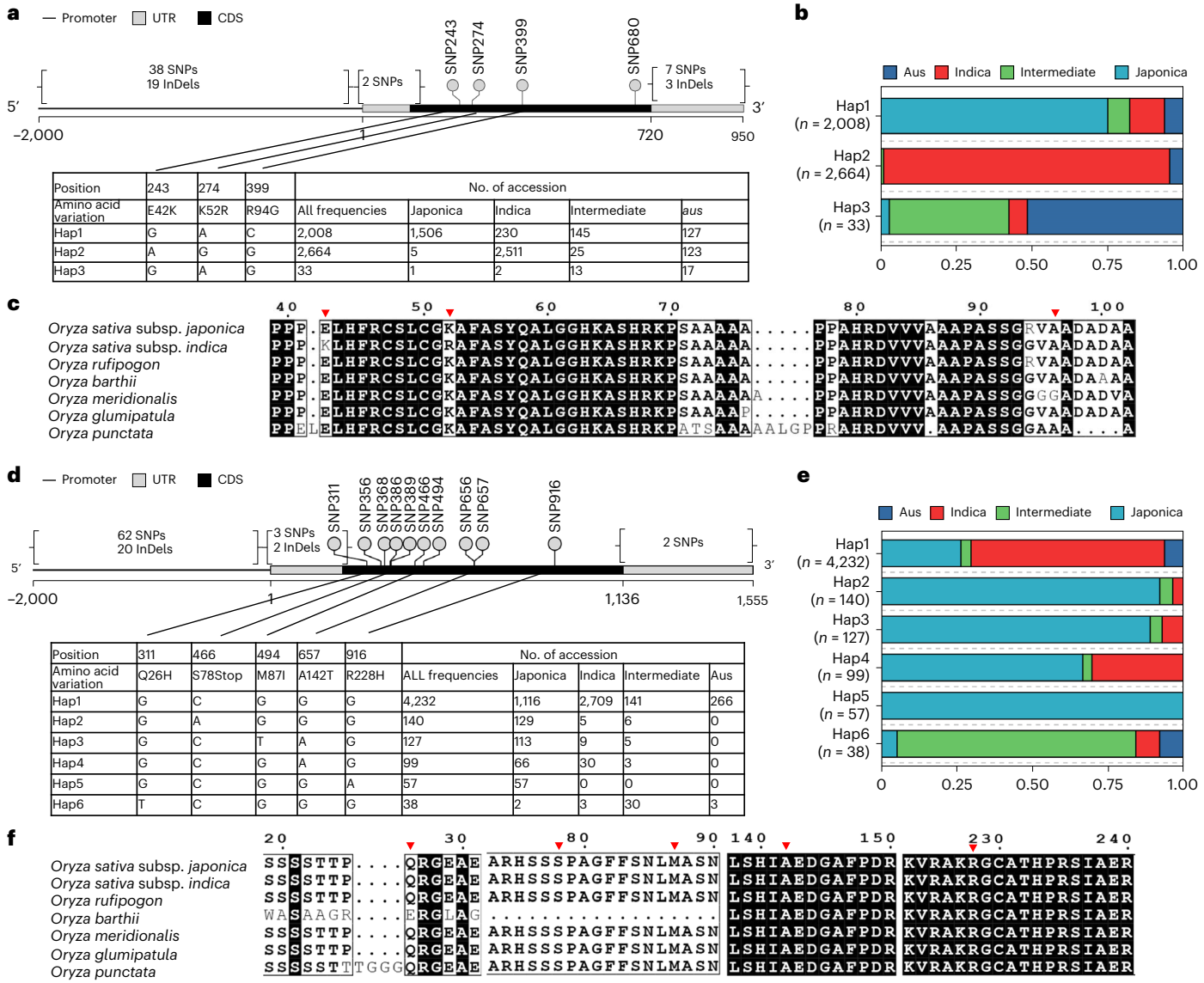

Position	243	274	399	No. of accession				
Amino acid variation	E42K	K52R	R94G	All frequencies	Japonica	Indica	Intermediate	*aus*
Hap1	G	A	C	2,008	1,506	230	145	127
Hap2	A	G	G	2,664	5	2,511	25	123
Hap3	G	A	G	33	1	2	13	17

Position	311	466	494	657	916	No. of accession				
Amino acid variation	Q26H	S78Stop	M87I	A142T	R228H	ALL frequencies	Japonica	Indica	Intermediate	Aus
Hap1	G	C	G	G	G	4,232	1,116	2,709	141	266
Hap2	G	A	G	G	G	140	129	5	6	0
Hap3	G	C	T	A	G	127	113	9	5	0
Hap4	G	C	G	A	G	99	66	30	3	0
Hap5	G	C	G	G	A	57	57	0	0	0
Hap6	T	C	G	G	G	38	2	3	30	3

Fig. 7 | *NAT1* and *bHLH110* have nonsynonymous natural variations. **a**–**f**, Natural variations analysis of 4,726 rice accessions for *NAT1* (**a**,**b**) and *bHLH110* (**d**,**e**). Nonsynonymous SNPs in the CDS region were classified into different haplotypes, and their ratio in different subtypes of rice was calculated. Hap1 represents the NPB (reference) allele. The number of SNPs and InDels in promoter and UTR regions is shown (**a**,**d**), and their variation details are in Supplementary Data 2. Protein multiple sequences were aligned for two rice subspecies (*japonica*, NPB; *indica*, 9311) and five wild rice species (**c**,**f**). Red arrowhead marks the site of nonsynonymous mutations in cultivated rice.

in rice (Fig. 8y). Furthermore, we have demonstrated the potential of modern gene-editing technology to edit a stress-induced negative regulator, thereby enhancing yield production in rice under heat stress conditions but without obvious yield penalty under normal growth conditions.

The plant cuticle is a hydrophobic barrier composed of cutin and cuticular wax[25]. Cutin is a polyester made up of hydroxy and epoxy fatty acids, while cuticular wax consists of very long-chain fatty acids, aldehydes, alkanes, ketones, alcohols and wax esters[26,27]. Several enzymes involved in wax biosynthesis have been identified[21,27,28], and the transcription factors WR1/WR2 positively regulate the expression of wax biosynthetic genes[11]. In this study, we found that the bHLH-type transcription factor bHLH110 is a positive regulator of *CER1*/*CER1L*, which is involved in the conversion of long-chain aldehydes to alkanes, a key step in wax biosynthesis. Other genes related to wax biosynthesis are also mis-expressed in *nat1-1* mutants, highlighting the important role of bHLH110 in wax biosynthesis and its association with thermotolerance in rice. Previous research has shown that TT2, the γ subunit of the heterotrimeric GTP-binding protein (G protein) complex, activates calmodulin 2 in response to heat stress[11]. TT2 inhibits the activity of two calmodulin-binding transcriptional activators, SCT1/SCT2, which are involved in wax biosynthesis, by promoting the expression of *WR2* (ref. 11). In contrast, in our study, we found that the expression of *TT2*/*SCT1*/*SCT2* remained unchanged in *NAT1*/*bHLH110* mutants and *NAT1*/*bHLH110* overexpression plants, suggesting that the NAT1–bHLH110–CER1/CER1L pathway identified here is distinct from the previously reported TT2–SCT1/SCT2–WR2 pathway. However, the expression of *WR2* is decreased in the *bhlh110* mutant and increased in *bHLH110* overexpression plants. Furthermore, it was found that bHLH110, rather than NAT1, directly binds to the *WR2* promoter and activates its activity in effector–reporter assays, suggesting a collaborative effort between these two pathways in regulating wax biosynthesis in rice, particularly in response to heat stress. Given that NAT1 and bHLH110 are transcription factors with potential multiple targets, further research into the functions of additional targets of NAT1/bHLH110 will be essential to gain a comprehensive

https://doi.org/10.1038/s41588-024-02065-2

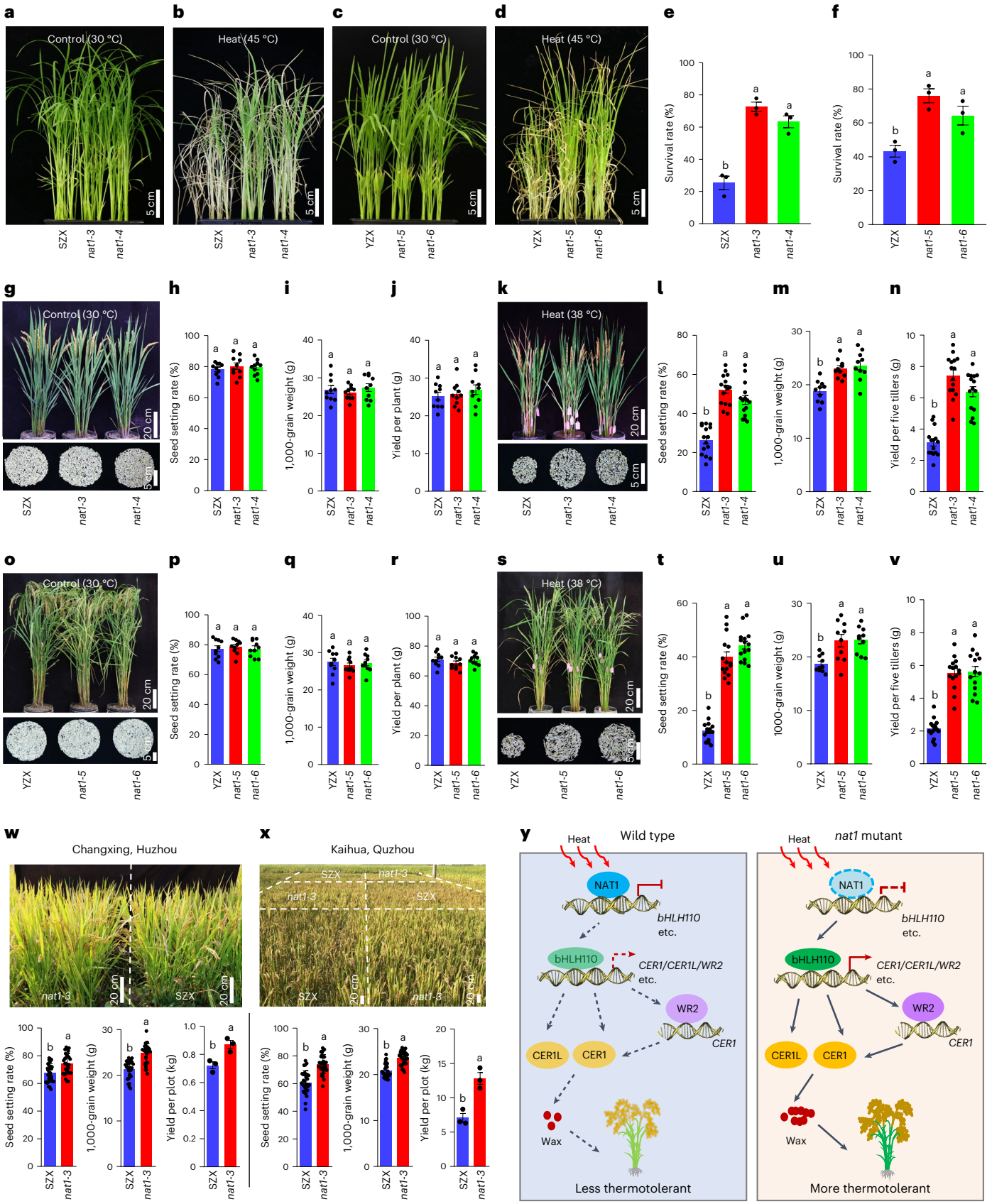

understanding of the thermotolerance mechanism mediated by NAT1/bHLH110.

Cuticular wax is believed to protect plants from excessive water loss during drought conditions[29,30] and acts as a physical barrier against invading pathogens and insect herbivores[26]. In our current study, we have confirmed that wax deposition also has a vital role in enhancing thermotolerance in rice. High temperatures stimulate plant transpiration rates, creating a trade-off between cooling leaves through

Fig. 8 | Improving thermotolerance in rice by editing *NAT1* without yield penalty. a–**v**, Phenotypic analysis. For the survival test, wild-type (SZX or YZX), *nat1* mutants in SZX background (*nat1-3*/*nat1-4*) or in YZX background (*nat1-5*/*nat1-6*) were subjected to heat stress (45 °C) for 2 days and then recovered at 30 °C, and the survival rate was then calculated (**a**–**f**). For the thermotolerance test at the reproductive stage, SZX/YZX, *nat1-3*/*nat1-4* and *nat1-5*/*nat1-6* were subjected to heat stress (38 °C) for 3 days during flowering and then recovered at 30 °C until maturity (**g**–**v**). The filled grains per plant (**g**,**o**) or per five panicles (**k**,**s**) were photographed and recorded. **w**,**x**, Field trials in two locations in Zhejiang province. SZX and *nat1-3* plants were grown in the field in Changxing, Huzhou (**w**) or in Kaihua, Quzhou (**x**). Data are presented as mean ± s.e.m., $n = 3$ in **e**,**f**; $n = 10$ in **h**–**j**,**p**–**r**; $n = 15$ in **l**–**n**,**t**–**v**; $n = 30$ for seed-setting rate and 1,000-grain weight and $n = 3$ for yield per plot in **w** and **x**. Different letters indicate significant differences between the two samples, as determined by the HSD test ($P < 0.05$) after two-way ANOVA analysis. Scale bars = 5 cm in **a**–**d** for plant heights and **g**,**k**,**o**,**s** for grains; 20 cm in **g**,**k**,**o**,**s**,**w**,**x** for plant heights. **y**, A working model for the thermotolerance conferred by *nat1* mutation. Under heat stress conditions, in the wild-type plants (left), NAT1 represses the expression of *bHLH110*, which effectively inhibits the bHLH110-mediated expression of *CER1*/*CER1L*/*WR2*. Both *CER1* and *CER1L* have a crucial role in wax biosynthesis. In contrast, in the gene-edited *nat1* mutant (right), the absence of *NAT1* repression allows for a significant increase in bHLH110 expression. Consequently, this leads to a higher expression level of *CER1*/*CER1L*/*WR2*, resulting in greater deposition of wax and enhanced thermotolerance during both the seedling and reproductive stages. WR2 also promotes the expression of *CER1*. Other target genes of NAT1/bHLH110 may also contribute to the conferred thermotolerance in *nat1* mutant plants.

excessive transpiration and conserving water by inhibiting transpiration[31]. ERECTA (ER), a leucine-rich repeat receptor-like kinase, is a key regulator of transpiration efficiency in *Arabidopsis*[32]. By overexpressing the *Arabidopsis ER* gene in rice and tomato, increased thermotolerance has been conferred through reduced transpiration[33]. Additionally, stomata aperture controls water transpiration efficiency through drought and salt tolerance-mediated H_2O_2 homeostasis[34,35]. The RING finger ubiquitin E3 ligase heat tolerance at the seedling stage (HTAS) enhances thermotolerance by modulating H_2O_2-induced stomatal closure, potentially preventing excessive transpiration[36]. In our study, we demonstrate that editing the *NAT1* gene locus leads to increased wax deposition and improved thermotolerance during both the seedling and reproductive stages. This highlights the importance of minimizing water loss under heat stress conditions to enhance thermotolerance.

Due to its low basal expression level, the *nat1* mutants do not exhibit growth or developmental defects under normal temperature conditions. This shows the potential to enhance abiotic stress tolerance without causing noticeable yield loss under normal growth conditions by targeting stress-induced negative regulators. Given that NAT1 is conserved in other crops such as maize, sorghum and wheat (Supplementary Fig. 32), which are also facing heat stresses[37], the identification of the NAT1–bHLH110–CER1/CER1L regulatory module presents a valuable opportunity for breeding high-temperature-resilient crops using gene-editing-assisted modern technology.

Online content

Any methods, additional references, Nature Portfolio reporting summaries, source data, extended data, supplementary information, acknowledgements, peer review information; details of author contributions and competing interests; and statements of data and code availability are available at https://doi.org/10.1038/s41588-024-02065-2.

References

1. Tilman, D., Balzer, C., Hill, J. & Befort, B. L. Global food demand and the sustainable intensification of agriculture. *Proc. Natl Acad. Sci. USA* **108**, 20260–20264 (2011).
2. Lobell, D. B., Schlenker, W. & Costa-Roberts, J. Climate trends and global crop production since 1980. *Science* **333**, 616–620 (2011).
3. Lesk, C., Rowhani, P. & Ramankutty, N. Influence of extreme weather disasters on global crop production. *Nature* **529**, 84–87 (2016).
4. Li, J. Y., Yang, C., Xu, J., Lu, H. P. & Liu, J. X. The hot science in rice research: how rice plants cope with heat stress. *Plant Cell Environ.* **46**, 1087–1103 (2023).
5. Sun, J. L., Li, J. Y., Wang, M. J., Song, Z. T. & Liu, J. X. Protein quality control in plant organelles: current progress and future perspectives. *Mol. Plant* **14**, 95–114 (2021).
6. Zhang, J. Y., Li, X. M., Lin, H. X. & Chong, K. Crop improvement through temperature resilience. *Annu. Rev. Plant Biol.* **70**, 753–780 (2019).
7. Kan, Y., Mu, X. R., Gao, J., Lin, H. X. & Lin, Y. The molecular basis of heat stress responses in plants. *Mol. Plant* **16**, 1612–1634 (2023).
8. Zhang, H. et al. A genetic module at one locus in rice protects chloroplasts to enhance thermotolerance. *Science* **376**, 1293–1300 (2022).
9. Li, J. & Liu, J. TT3.1: a journey to protect chloroplasts upon heat stress. *Stress Biol.* **2**, 27 (2022).
10. Liu, X. H. et al. A membrane-associated NAC transcription factor OsNTL3 is involved in thermotolerance in rice. *Plant Biotechnol. J.* **18**, 1317–1329 (2020).
11. Kan, Y. et al. TT2 controls rice thermotolerance through SCT1-dependent alteration of wax biosynthesis. *Nat. Plants* **8**, 53–67 (2022).
12. Li, X. M. et al. Natural alleles of a proteasome α2 subunit gene contribute to thermotolerance and adaptation of African rice. *Nat. Genet.* **47**, 827–833 (2015).
13. Islam, M. A., Du, H., Ning, J., Ye, H. & Xiong, L. Characterization of *Glossy1*-homologous genes in rice involved in leaf wax accumulation and drought resistance. *Plant Mol. Biol.* **70**, 443–456 (2009).
14. Sugio, A., Dreos, R., Aparicio, F. & Maule, A. J. The cytosolic protein response as a subcomponent of the wider heat shock response in *Arabidopsis*. *Plant Cell* **21**, 642–654 (2009).
15. Guo, M. et al. The plant heat stress transcription factors (HSFs): structure, regulation, and function in response to abiotic stresses. *Front. Plant Sci.* **7**, 114 (2016).
16. Zhang, S. S. et al. Tissue-specific transcriptomics reveals an important role of the unfolded protein response in maintaining fertility upon heat stress in *Arabidopsis*. *Plant Cell* **29**, 1007–1023 (2017).
17. He, Y. B. et al. Programmed self-elimination of the *CRISPR/Cas9* construct greatly accelerates the isolation of edited and transgene-free rice plants. *Mol. Plant* **11**, 1210–1213 (2018).
18. Arshad, M. S. et al. Thermal stress impacts reproductive development and grain yield in rice. *Plant Physiol. Biochem.* **115**, 57–72 (2017).
19. Kagale, S. & Rozwadowski, K. EAR motif-mediated transcriptional repression in plants: an underlying mechanism for epigenetic regulation of gene expression. *Epigenetics* **6**, 141–146 (2011).
20. Aarts, M. G. M., Keijzer, C. J., Stiekema, W. J. & Pereira, A. Molecular characterization of the *CER1* gene of *Arabidopsis* involved in epicuticular wax biosynthesis and pollen fertility. *Plant Cell* **7**, 2115–2127 (1995).
21. Ni, E. et al. OsCER1 plays a pivotal role in very-long-chain alkane biosynthesis and affects plastid development and programmed cell death of tapetum in rice (*Oryza sativa* L.). *Front. Plant Sci.* **9**, 1217 (2018).
22. Persikov, A. V. & Singh, M. De novo prediction of DNA-binding specificities for Cys_2His_2 zinc finger proteins. *Nucleic Acids Res.* **42**, 97–108 (2014).
23. Kovach, M. J., Sweeney, M. T. & McCouch, S. R. New insights into the history of rice domestication. *Trends Genet.* **23**, 578–587 (2007).

24. Huang, X. et al. A map of rice genome variation reveals the origin of cultivated rice. *Nature* **490**, 497–501 (2012).
25. Yeats, T. H. & Rose, J. K. C. The formation and function of plant cuticles. *Plant Physiol.* **163**, 5–20 (2013).
26. Lewandowska, M., Keyl, A. & Feussner, I. Wax biosynthesis in response to danger: its regulation upon abiotic and biotic stress. *New Phytol.* **227**, 698–713 (2020).
27. Lee, S. B. & Suh, M. C. Regulatory mechanisms underlying cuticular wax biosynthesis. *J. Exp. Bot.* **73**, 2799–2816 (2022).
28. Ni, E. et al. OsCER1 regulates humidity-sensitive genic male sterility through very-long-chain (VLC) alkane metabolism of tryphine in rice. *Funct. Plant Biol.* **48**, 461–468 (2021).
29. Wang, Z. et al. The E3 ligase drought hypersensitive negatively regulates cuticular wax biosynthesis by promoting the degradation of transcription factor ROC4 in rice. *Plant Cell* **30**, 228–244 (2018).
30. Jian, L., Kang, K., Choi, Y., Suh, M. C. & Paek, N. C. Mutation of *OsMYB60* reduces rice resilience to drought stress by attenuating cuticular wax biosynthesis. *Plant J.* **112**, 339–351 (2022).
31. Sadok, W., Lopez, J. R. & Smith, K. P. Transpiration increases under high-temperature stress: potential mechanisms, trade-offs and prospects for crop resilience in a warming world. *Plant Cell Environ.* **44**, 2102–2116 (2021).
32. Masle, J., Gilmore, S. R. & Farquhar, G. D. The *ERECTA* gene regulates plant transpiration efficiency in *Arabidopsis*. *Nature* **436**, 866–870 (2005).
33. Shen, H. et al. Overexpression of receptor-like kinase *ERECTA* improves thermotolerance in rice and tomato. *Nat. Biotechnol.* **33**, 996–1003 (2015).
34. Huang, X. Y. et al. A previously unknown zinc finger protein, DST, regulates drought and salt tolerance in rice via stomatal aperture control. *Genes Dev.* **23**, 1805–1817 (2009).
35. Ding, Y. F. et al. Rice DST transcription factor negatively regulates heat tolerance through ROS-mediated stomatal movement and heat-responsive gene expression. *Front. Plant Sci.* **14**, 1068296 (2023).
36. Liu, J. et al. The RING finger ubiquitin E3 ligase OsHTAS enhances heat tolerance by promoting H_2O_2-induced stomatal closure in rice. *Plant Physiol.* **170**, 429–443 (2016).
37. Prasad, P. V. V., Bheemanahalli, R. & Jagadish, S. V. K. Field crops and the fear of heat stress—opportunities, challenges and future directions. *Field Crops Res.* **200**, 114–121 (2017).

Methods

Plant materials and phenotypic analysis

Three wild-type plants (subsp. NPB, SZX and YZX) were used in the current study. To generate the transgene-free gene-edited mutant plants, gene-specific guide sequences (sgRNAs) for *NAT1* (LOC_Os07g40080), *bHLH110* (LOC_Os02g39140), *CER1* (LOC_Os02g40784) and *CER1L* (LOC_Os02g56920) were designed and cloned into the CRISPR–Cas9 system[17]. To obtain the overexpression plants, full-length CDs of *NAT1* and *bHLH110* were amplified and cloned into the vectors pCAMBIA1300-MYC and pCAMBIA1300-FLAG, respectively. Error-free constructs were used to generate transgenic rice plants via the *Agrobacterium*-mediated stable transformation. All the primers are included in the Supplementary Table 1. For checking the expression level of transgenes, antibodies (Abmart; 1:5,000) of anti-MYC, anti-FLAG, anti-β-tubulin and secondary antibody goat anti-mouse IgG-HRP (Abmart; 1:10,000) were used in western blot analysis.

To conduct the phenotypic analysis at the seedling stage, rice seedlings were cultivated in Kimura B nutrient solution under 20,000 lux light conditions (12-h light/12-h dark) within growth chambers (CONVIRON PGR15). Heat stress was induced by transferring 7-day-old plants grown at 30 °C to the growth chambers with a temperature setting of 45 °C for 2 days. Subsequently, the plants were returned to the growth chamber at 30 °C for 7 days to recover. Representative plants were photographed, and the survival rate was calculated in each experiment with every replicate consisting of 24 plants.

For the phenotypic analysis at the reproductive stage, plants were grown at 30 °C until heading, and tillers/panicles in a similar developmental stage were selected by tagging them, and rice plants were subjected to heat stress (38 °C) in the growth chamber for 3 days. They were then allowed to recover at 30 °C until maturity. Representative plants were photographed, and seed-setting rate and grain yield were then measured for the tagged tillers.

Field tests were conducted at Changxing, Huzhou (longitude = 119.9, latitude = 31.0), or Kaihua, Quzhou (longitude = 118.4, latitude = 29.1) in Zhejiang province. A randomized block design with three replicates was used. There were 25 plants per plot (1 m^2) in Huzhou and 225 plants per plot (9 m^2) in Kaihua, respectively. The border plants were also grown to avoid margin effects. At maturity, grain yield was calculated on a per-plot basis, and seed set rates were determined on a per-plant basis. Measurements were taken from distinct samples for all the experiments.

Subcellular localization study

For protein subcellular localization studies, the CDs of *NAT1*, or *bHLH110*, were amplified and subcloned into the pCAMBIA1300-GFP vector. These C-terminal GFP-tagged fusion proteins were transiently co-expressed with the nuclear protein marker (NLS-mCherry) in tobacco (*Nicotiana benthamiana*) epidermal leaves and observed under confocal microscopy (Zeiss LSM A710). All the primers are listed in Supplementary Table 1.

Effector–reporter assays

For effector–reporter assays, the promoter sequence of bHLH110/WR2/CER1/CER1L or synthesized *cis*-elements were inserted into the pGreen0800-II vector together with the 35S promoter or 35S minimal promoter to generate the firefly luciferase reporter, and the Renilla luciferase driven by the 35S promoter served as an internal control. The CDS of NAT1 or bHLH110 or WR2 was inserted into the pCAMBIA1300-MYC or pCAMBIA1300-FLAG vector to generate the effector vector. Different combinations of constructs were transiently expressed in tobacco leaves, and the luciferase activity was measured with a dual-luciferase reporter assay kit (Promega). Relative luciferase activity is the firefly luciferase activity normalized to the Renilla luciferase activity (internal control), which was then normalized to the vector control (LexA-BD). All the primers are listed in Supplementary Table 1.

Gene expression analysis

For RNA-seq analysis, 7-day-old rice NPB and *nat1-1* seedlings grown at 30 °C were subjected to heat stress (45 °C) for 1 h and then harvested for RNA-seq analysis using an Illumina HiSeq 4000 (LC-Bio Technologies) following the standard Illumina protocols[38]. Clean reads were aligned to the reference genome with the HISAT2 (https://daehwankimlab.github.io/hisat2/, version: hisat2-2.2.1) package, and StringTie (http://ccb.jhu.edu/software/stringtie/, version: stringtie-2.1.6) was used to assemble the mapped reads with default parameters. The expression level of each gene was normalized to fragment per kilobase of transcript per million mapped reads value. Differential gene expression analysis was compared with DESeq2 (v1.40.2) between two groups and edgeR (v3.42.4) between two samples. Differentially upregulated genes were defined with the cutoff—$q < 0.05$, fold change (FC) ≥ 2 and downregulated genes with $q < 0.05$, FC < 0.5. KEGG analysis was performed using clusterProfiler (v4.2.2) software, the top 20 pathways were screened out according to the *P* values and a bubble chart was drawn with ggplot2 (v3.5.1) software at the OmicStudio cloud platform provided by LC-Bio Technology. The default statistical setting was two-sided, and no adjustment was made.

For RT–qPCR, total RNA was extracted using a RAN Prep Pure Plant Kit (Tiangen) and reverse-transcribed with the 5× PrimeScript RT Master Mix (Takara) and oligo (d*T*) primers (Takara). RT–qPCR was run in the CFX96 real-time system (Bio-Rad) using the SuperReal PreMix Plus Kit (Tiangen). The ΔΔCt (threshold cycle) method was used for the calculation. Relative expression is the expression of the target gene normalized to that in NPB at 30 °C, both of which were normalized to that of *PP2A*. All the primers are listed in Supplementary Table 1.

In situ hybridization

Digoxigenin-uridine triphosphate (UTP)-labeled sense and antisense probes were synthesized by in vitro transcription using T7 RNA polymerase (Roche). In situ hybridizations were performed following previous protocols[39]. Stem cross-sections were deparaffinized with xylene for 10 min twice, rehydrated in 100%, 90%, 70%, 50% and 30% ethanol series and diethyl pyrocarbonate (DEPC)-treated water for 2 min each, followed by proteinase K (Takara) at 37 °C for 40 min and refixation in 4% (wt/vol) formaldehyde for 60 min. Hybridization was performed at 50 °C without probe for 2 h in prehybridization buffer (50% formamide, 5× saline-sodium citrate (SSC), 0.92 mM citric acid, 0.1% Tween-20, 50 μg ml^{-1} heparin (Sigma) and 1 mg ml^{-1} tRNA (Sigma)). Subsequently, 500 ng ml^{-1} probe was added at 50 °C overnight. On the second day, slides were washed with 2× SSCT (2× SSC, 0.92 mM citric acid, 0.2% Tween-20)/50% formamide, 2× SSCT/25% formamide, 2× SSCT and 0.2× SSCT for 20 min each time. Sections were incubated in blocking solution (10% phosphate buffered saline with Tris (PBST) for 2 h at room temperature and then incubated with antidigoxigenin-AP antibodies (Roche; 1:5,000) for 2 h at room temperature. After washing with PBST three times (30 min each), samples were equilibrated with detection buffer (100 mM Tris–HCl (pH 9.5), 50 mM or 5 mM $MgCl_2$, 100 mM NaCl and 0.1% Tween-20) three times (30 min each), and color was developed with tetranitroblue tetrazolium chloride (NBT)/5-bromo-4-chloro-3-indolyl phosphate disodium salt (BCIP) (Beyotime) in the dark.

ChIP–qPCR

ChIP assays were carried out according to standard methods. Briefly, 7-day-old *NAT1-MYC* or *bHLH110-FLAG* overexpression plants were sampled for fixation with 1% formaldehyde for 15 min, which was stopped by adding 0.15 M glycine. Nuclei were extracted and resuspended in a lysis buffer. After sonication in 0.8% SDS buffer, the mix was immunoprecipitated with anti-MYC (Abmart) or anti-FLAG antibody (Abmart) or anti-GST (Abmart) as the IgG control. qPCR was performed with routine procedures.

EMSA

The full-length CDS of NAT1 and bHLH110 were cloned into the pET28a and pETMAL-H vectors, respectively. The fusion proteins, NAT1-His and

bHLH110-MBP, were expressed in BL21 cells and then extracted and purified for EMSA. The 3′ ends of probes used for EMSA were labeled with biotin according to the Biotin 3′ End DNA Labeling Kit (Thermo Fisher Scientific). EMSA was performed using a Light Shift Chemiluminescent EMSA Kit (Thermo Fisher Scientific). Briefly, each binding reaction (20 mM HEPES (pH 7.2), 80 mM KCl, 0.1 mM EDTA, 10% glycerol, 2.5 mM DTT, 0.07 mg ml^{-1} BSA and 8 ng ml^{-1} poly dI-dC) was set at room temperature for 20 min and run on a 5% nondenaturing polyacrylamide gel. After transferring to a nylon membrane (GE), the blot was UV light cross-linked and detected with the chemiluminescent nucleic acid detection module (Thermo Fisher Scientific).

MST assays

The proteins GFP-His and NAT1–GFP-His were expressed in *BL21* using pET28a and purified with nickel column. Complementary pairs of oligonucleotides (same sequences as in EMSA) were annealed and added to the protein elution. An MST assay was performed using the Monolith NT.115 (NanoTemper Technologies). Samples were loaded into NT.115 premium capillaries. Measurements were performed at 21 °C, 80% LED, 20% infrared ray (IR)-laser power and at a constant concentration of 100 nM of protein with increasing concentration of purified oligonucleotides.

Scanning microscopy

Scanning electron microscopy was used to image the cuticular wax crystallization patterns. The fresh leaf sample was dried in a machine, Hitachi HCP-2, and coated with gold for 2 min in a sputter coater (Hitachi, MC1000) and viewed by a scanning electron microscope (Hitachi, SU-8010).

Wax content determination

The cuticular waxes were extracted by immersing the whole leaf for 30 s into 30 ml of chloroform at 60 °C. Heptadecanoic acid (C17:0) was added as an internal standard. The solvent was dried under a gentle stream of nitrogen and dissolved in 150 µl of N,O-bis(trimethylsilyl) trifluoroacetamide with trimethylchlorosilane (BSTFA–TMCS, 99:1) and then was derivatized at 110 °C for 30 min. After BSTFA–TMCS was evaporated, samples were solubilized in chloroform for qualitative analysis by GC–MS (Agilent gas chromatograph equipped with an HP-5MS column (30 m × 0.32 mm × 0.25 µm) and a flame ionization detector). The initial temperature of 50 °C was held for 4 min, increased by 7 °C per min to 300 °C and held for 5 min.

Natural variations and population genetic analysis

Homologous proteins of NAT1 or bHLH110 were obtained by using the UniProt database (https://www.uniprot.org/). Natural variation and haplotype analysis were carried out with the genotype data of 4,726 rice accessions downloaded from the RiceVarMap v.2.0 (https://ricevarmap.ncpgr.cn/). The VCF format file used for the population selection analysis, sourced from the 5,104 rice accessions[40], was processed using vcftools (v0.1.16) to calculate nucleotide diversity (π) and population differentiation index (F_{ST}) for the 2-Mb regions flanking *NAT1* and *bHLH110*, using a 50-kb window size with a 5-kb overlapping step size across the genome.

Statistics analysis and reproducibility

Data are presented as mean ± s.e.m. The exact numbers used to calculate the statistics are shown in each figure legend. StatView (v.5.0) was used for all statistical analysis. Two-sided *t*-test and two-way analysis of variance (ANOVA) were performed, and results with a P value < 0.05 were considered statistically significant. Experiments regarding the RNA in situ hybridization, confocal microscopy and scanning microscopy were repeated at least three times using tissues from different individual plants.

Reporting summary

Further information on research design is available in the Nature Portfolio Reporting Summary linked to this article.

Data availability

The RNA-seq data are deposited in the NCBI-SRA database (PRJNA1171028) and the Genome Sequence Archive database (CRA013469). All data supporting the findings of this study are available within the paper and its Supplementary Information. Source data are provided with this paper.

Code availability

All software used in the study are publicly available from the Internet as described in the Methods and Reporting Summary.

References

38. Yang, C., Luo, A., Lu, H. P., Davis, S. J. & Liu, J. X. Diurnal regulation of alternative splicing associated with thermotolerance in rice by two glycine-rich RNA-binding proteins. *Sci. Bull.* **69**, 59–71 (2024).
39. Yang, J. et al. Brassinosteroids modulate meristem fate and differentiation of unique inflorescence morphology in *Setaria viridis*. *Plant Cell* **30**, 48–66 (2018).
40. Xie, L. et al. Population genomic analysis unravels the evolutionary roadmap of pericarp color in rice. *Plant Commun.* **5**, 100778 (2024).

Acknowledgements

This project was financially supported by grants from the State Key Project of Research and Development Plan (2022YFF1001603 to J.-X.L.) and the Zhejiang Provincial Natural Science Foundation of China (LD21C020001 to J.-X.L.). We would like to thank S.-J. Lu for initiating the project, Z. Ma for technical assistance, X. Huang and L. Fan for advice on domestication analysis, and L.-M. Cao and J.-L. Huang for providing the SZX and YZX recipient seeds, respectively.

Author contributions

J.-X.L., H.-P.L., X.-H.L. and M.-J.W. designed the experiments. H.P.L., X.-H.L., M.-J.W., Q.-Y.Z., Y.-S.L. and J.-H.X. performed the experiments. J.-X.L. and H.-P.L. analyzed the data. J.-X.L. and H.-P.L. wrote the paper.

Competing interests

The authors declare no competing interests.

Additional information

Supplementary information The online version contains supplementary material available at https://doi.org/10.1038/s41588-024-02065-2.

Correspondence and requests for materials should be addressed to Jian-Xiang Liu.

Peer review information *Nature Genetics* thanks Weiqiang Qian and the other, anonymous, reviewer(s) for their contribution to the peer review of this work.

nature portfolio

Corresponding author(s): Jian-Xiang Liu

Last updated by author(s): Oct 11, 2024

Reporting Summary

Nature Portfolio wishes to improve the reproducibility of the work that we publish. This form provides structure for consistency and transparency in reporting. For further information on Nature Portfolio policies, see our Editorial Policies and the Editorial Policy Checklist.

Statistics

For all statistical analyses, confirm that the following items are present in the figure legend, table legend, main text, or Methods section.

n/a	Confirmed
☐	☒ The exact sample size (*n*) for each experimental group/condition, given as a discrete number and unit of measurement
☐	☒ A statement on whether measurements were taken from distinct samples or whether the same sample was measured repeatedly
☐	☒ The statistical test(s) used AND whether they are one- or two-sided *Only common tests should be described solely by name; describe more complex techniques in the Methods section.*
☒	☐ A description of all covariates tested
☒	☐ A description of any assumptions or corrections, such as tests of normality and adjustment for multiple comparisons
☐	☒ A full description of the statistical parameters including central tendency (e.g. means) or other basic estimates (e.g. regression coefficient) AND variation (e.g. standard deviation) or associated estimates of uncertainty (e.g. confidence intervals)
☐	☒ For null hypothesis testing, the test statistic (e.g. *F*, *t*, *r*) with confidence intervals, effect sizes, degrees of freedom and *P* value noted *Give P values as exact values whenever suitable.*
☒	☐ For Bayesian analysis, information on the choice of priors and Markov chain Monte Carlo settings
☒	☐ For hierarchical and complex designs, identification of the appropriate level for tests and full reporting of outcomes
☒	☐ Estimates of effect sizes (e.g. Cohen's *d*, Pearson's *r*), indicating how they were calculated

Our web collection on statistics for biologists contains articles on many of the points above.

Software and code

Policy information about availability of computer code

Data collection	RiceVarMap v.2.0 (https://ricevarmap.ncpgr.cn/)
Data analysis	HISAT2,v hisat2-2.2.1; StringTie, v stringtie-2.1.6; DESeq2, v 1.40.2; edgeR, v 3.42; clusterProfiler, v 4.2.2; ggplot2, v 3.5.1; vcftools, v 0.1.16; StatView, v 5.0..

For manuscripts utilizing custom algorithms or software that are central to the research but not yet described in published literature, software must be made available to editors and reviewers. We strongly encourage code deposition in a community repository (e.g. GitHub). See the Nature Portfolio guidelines for submitting code & software for further information.

Data

Policy information about availability of data

All manuscripts must include a data availability statement. This statement should provide the following information, where applicable:

- Accession codes, unique identifiers, or web links for publicly available datasets
- A description of any restrictions on data availability
- For clinical datasets or third party data, please ensure that the statement adheres to our policy

The RNA-seq data is deposited in the Genome Sequence Archive (GSA) database (CRA013469) and NCBI-SRA database (PRJNA1171028). Source data are provided with this paper. All data supporting the findings of this study are available within the paper and its Supplementary Information.

Research involving human participants, their data, or biological material

Policy information about studies with human participants or human data. See also policy information about sex, gender (identity/presentation), and sexual orientation and race, ethnicity and racism.

Reporting on sex and gender	N/A
Reporting on race, ethnicity, or other socially relevant groupings	N/A
Population characteristics	N/A
Recruitment	N/A
Ethics oversight	N/A

Note that full information on the approval of the study protocol must also be provided in the manuscript.

Field-specific reporting

Please select the one below that is the best fit for your research. If you are not sure, read the appropriate sections before making your selection.

☒ Life sciences ☐ Behavioural & social sciences ☐ Ecological, evolutionary & environmental sciences

For a reference copy of the document with all sections, see nature.com/documents/nr-reporting-summary-flat.pdf

Life sciences study design

All studies must disclose on these points even when the disclosure is negative.

Sample size	We followed sample size settings in literatures for preliminary field study, in each replicate, there were 25 plants per plot (1 m2) in Huzhou and 225 plants per plot (9 m2) in Kaihua, respectively.
Data exclusions	No data is excluded.
Replication	There were three replications, all attempts at replications were successful, and no data was excluded.
Randomization	All plots were randomly placed in the same field and all data was collected in each experiment.
Blinding	Blinded.

Reporting for specific materials, systems and methods

We require information from authors about some types of materials, experimental systems and methods used in many studies. Here, indicate whether each material, system or method listed is relevant to your study. If you are not sure if a list item applies to your research, read the appropriate section before selecting a response.

Materials & experimental systems

n/a	Involved in the study
☐	☒ Antibodies
☒	☐ Eukaryotic cell lines
☒	☐ Palaeontology and archaeology
☒	☐ Animals and other organisms
☒	☐ Clinical data
☒	☐ Dual use research of concern
☐	☒ Plants

Methods

n/a	Involved in the study
☒	☐ ChIP-seq
☒	☐ Flow cytometry
☒	☐ MRI-based neuroimaging

Antibodies

Antibodies used	anti-MYC Mouse mAb, Abmart; Cat#M20002L; RRID: AB_2861172; 1:5000 anti-FLAG Mouse Ab, Abmart; Cat#M20008H; RRID: AB_2713960; 1:5000 anti-b-Tubulin Mouse Ab, Abmart; Cat#M30109L; RRID: AB_2916070; 1:5000

anti-digoxigenin-AP Ab, Roche; Cat#11093274910; RRID: 57696520; 1:5000
Goat anti-mouse IgG-HRP Ab, Abmart; Cat#M21001L; RRID: AB_2713950; 1:10000

Validation

These commercial antibodies have been validated and widely used in literatures.

Dual use research of concern

Policy information about dual use research of concern

Hazards

Could the accidental, deliberate or reckless misuse of agents or technologies generated in the work, or the application of information presented in the manuscript, pose a threat to:

No	Yes	
☒	☐	Public health
☒	☐	National security
☒	☐	Crops and/or livestock
☒	☐	Ecosystems
☒	☐	Any other significant area

Experiments of concern

Does the work involve any of these experiments of concern:

No	Yes	
☒	☐	Demonstrate how to render a vaccine ineffective
☒	☐	Confer resistance to therapeutically useful antibiotics or antiviral agents
☒	☐	Enhance the virulence of a pathogen or render a nonpathogen virulent
☒	☐	Increase transmissibility of a pathogen
☒	☐	Alter the host range of a pathogen
☒	☐	Enable evasion of diagnostic/detection modalities
☒	☐	Enable the weaponization of a biological agent or toxin
☒	☐	Any other potentially harmful combination of experiments and agents

Plants

Seed stocks

N/A

Novel plant genotypes

To generate the transgene-free gene-edited mutant plants, gene-specific guide sequences (sgRNAs) for NAT1 (LOC_Os07g40080), bHLH110 (LOC_Os02g39140), CER1 (LOC_Os02g40784), and CER1L (LOC_Os02g56920) were designed and cloned into the CRISPR/Cas9 system. To obtain the overexpression plants, full-length coding sequences of NAT1 and bHLH100 were amplified and cloned into the vector pCAMBIA1300-MYC and pCAMBIA1300-FLAG, respectively. Error-free constructs were used to generate transgenic rice plants via the Agrobacterium-mediated stable transformation.

Authentication

N/A